

Response to review of “The spectral signature of cloud spatial structure in shortwave irradiance” by anonymous Referee #1

Sebastian Schmidt, corresponding author

We very much appreciate the thorough and positive review of this manuscript and the helpful comments for improving content, clarity, and context within the literature. We are open for further input, should we have mis-interpreted the reviewer’s points (point-by-point response below).

Assessment by reviewer: Minor revisions

General points:

#1 Even though this paper contains plentiful new findings and scientific discussions, I feel that the manuscript lacks coherence. I believe that the manuscript can be significantly improved if the authors rearrange paragraphs and shorten unnecessary explanations in Introduction and Discussions.

We agree with the reviewer and heeded the advice by removing unnecessary explanations (not just in the introduction), especially the ones pertaining to radiances, which interrupted the flow of the paper. It was tempting to allude to this topic in this paper, but we realize that it is better addressed in a companion paper. Rather than going into too much detail here, we instead included a reference to a Ph.D. and the companion paper (Song et al. 2016, to be submitted soon). Changes are highlighted in the revised version of this paper. Most of the changes in response to this comment are in the introduction and in the body of the paper; the Summary & Conclusions section was shortened only slightly because we felt the need to discuss the significance of our findings given the unusually large amount of material covered, and this was appreciated by reviewer #2.

References:

Song, 2016: The Spectral Signature of Cloud Spatial Structure in Shortwave Radiation, *Ph.D. thesis, University of Colorado at Boulder*.

Song, S., K. S. Schmidt, Pilewskie, P., King, M. D., Platnick, S., 2016: Quantifying the spectral signature of heterogeneous clouds in shortwave radiance and irradiance measurements, to be submitted to *JGR SEAC⁴RS special issue*

#2 This manuscript clearly showed a reliable relationship between horizontal net transport and spectral dependency, built a parameterization function, and solved coefficients of the function, such as ϵ . This is an excellent work indeed. However, it is also important to give a specific direction how the users can apply the parameterization method for inferring 3D effects. I think this is briefly discussed in Section 9 (page 23, line 4-23), so the authors can simply add more detailed explanation/justification of the parameterization in Sections 6 or 9.

This is a very good point, which was brought up by both reviewers. Indeed, the term “parameterization” might suggest that it can be exploited for inferring, simplifying, or correcting 3D effects, and the authors are currently working on this very topic. However, the parameterization is only the first step towards this goal, and it cannot (yet) be translated into such immediate practical applications, although this is certainly the goal for the future. The purpose of the parameterization is to capture the relationship between net horizontal photon transport and its spectral dependence using one main parameter (ϵ). The companion paper (Song et al., 2016) will look at the connections between 3D effects on irradiances and radiances. We will include this explanation in the revised version. For example, we conclude the abstract with the following statement: “Since three-dimensional effects depend on the spatial context of a given pixel in a non-trivial way, the spectral dimension of this problem may emerge as the starting point for future bias corrections.” In section 6, we included this statement “Although our study was instigated by aircraft measurements, its findings are also relevant for satellite-based derivations of cloud radiative effects since the spectral perturbations $d\lambda$ propagate into observed radiances (Song et al., 2016). This may be exploited in future applications for deriving correction terms for 3D radiative effects via their spectral signature.” We hope this clarifies the purpose of the parameterization.

#3 As also commented in the manuscript, the relationship between H and S was inferred in Schmidt et al. (2010). In my understanding, the paper definitely shows new findings, such as a strong linear relationship on a pixel-basis, confirmation of molecular effects from the sensitivity study, and parameterization for the future applications. If this paper highlights new findings in Abstract and Introduction clearly, the readers would catch them more easily.

We agree – it was somewhat unclear in the abstract what was done in earlier studies vs. this paper. The revised abstract was re-structured significantly, and clearly points out the new aspects of this paper at the very beginning, i.e., identifying the physical mechanism that causes the correlation between spatial structure and spectral signature, as well as the parameterization developed on its basis. The new abstract reads as follows:

“In this paper, we used cloud imagery from a NASA field experiment in conjunction with three-dimensional radiative transfer calculations to show that cloud spatial structure manifests itself as spectral signature in shortwave irradiance fields – specifically in transmittance and net horizontal photon transport in the visible and near-ultraviolet wavelength range. We found a robust correlation between the magnitude of net horizontal photon transport (H) and its spectral dependence (slope), which is scale-invariant and holds for the entire pixel population of a domain. This was at first surprising given the large degree of spatial inhomogeneity, but seems to be valid for any cloud field. We prove that the underlying physical mechanism for this phenomenon is molecular scattering in conjunction with cloud inhomogeneity. On this basis, we developed a simple parameterization through a single parameter ϵ , which quantifies the characteristic spectral signature of spatial heterogeneities. In the case we studied, neglecting net horizontal photon transport leads to a transmittance bias of ± 12 - 19% even at the relatively coarse spatial resolution of 20 kilometers. Since three-dimensional effects depend on the spatial

context of a given pixel in a non-trivial way, the spectral dimension of this problem may emerge as the starting point for future bias corrections.”

Specific points:

#1 In Abstract, it might be necessary to comment significance of 3D effects, but the authors can simply mention it here and discuss in more detail in later sections. It seems this long discussion hinders main points of this paper (the strong linear relationship that authors found and devise a parameterization method).

Agreed; see the point above along with the modified abstract. The discussion of 3D effects for the particular case studied in our paper was moved to the end, to emphasize the main points (presented at the beginning).

#2 Line 1, Page 2: It is not clear what spectral radiance perturbation means. Please explain spectral radiance perturbation, or remove the last sentence of Abstract.

The last sentence of the abstract was deleted, and a more general statement was added (“Since three-dimensional effects depend on the spatial context of a given pixel in a non-trivial way, the spectral dimension of this problem may emerge as the starting point for future bias corrections.”).

#3 Line 5-10, Page 3: “The spectral dependence” and the following sentence, I am not sure why the fact - $|H|$ at visible band is similar to $|A|$ at near-infrared - is related to significance of H in broadband A . These two sentences do not seem cause and effect. Please revise them.

We revised this section on page 3 to address this problem, it now reads as follows:

“Schmidt et al. (2010) derived *apparent absorption*, the sum of A and H , from irradiance measurements aboard the NASA ER-2 and DC-8 aircraft that flew along a collocated path above and below a heterogeneous anvil cloud during the Tropical Composition, Cloud and Climate Coupling Experiment (TC⁴) (Toon et al., 2010). The results of this study showed that, in absolute terms, H at visible wavelengths (where cloud and gas absorption are negligible) can attain a similar magnitude as the absorbed irradiance A at near-infrared wavelengths. Horizontal photon transport thus has the potential to mimic substantially enhanced absorption. Three-dimensional (3D) calculations confirmed the measurements, and radiative closure was achieved within measurement and model uncertainties without invoking proposed enhanced gas absorption (Arking, 1999) or big cloud droplets (Wiscombe et al., 1984).”

Note that we kept the statement “Horizontal photon transport thus has the potential to mimic substantially enhanced absorption,” but removed the term “broadband”. What we meant was that a broadband observation of “absorption” by way of collocated legs above

and below a cloud layer is really the wavelength integral of $A_{\lambda} + H_{\lambda}$, not just A_{λ} . If the magnitude of H in the visible is on the same order of magnitude as A in the near-infrared, the contribution of H to the broadband integral of $A+H$ may be comparable to that of A . In fact, it may even outweigh it (not stated in the paper). For this reason, it is important to make spectrally resolved measurements; otherwise it is impossible to separate H and A (in the spirit of the Ackerman & Cox papers).

#4 The authors often used footnotes. However, ACP does not recommended foot- notes because they disrupt the flow of text. Please consider removing footnotes and includes them in the main text. Please refer to http://www.atmospheric-chemistry-and-physics.net/for_authors/manuscript_preparation.html .

Thank you, all the footnotes were either removed (where not of central importance to the manuscript) or incorporated into the manuscript.

#5 Line 6-9, Page 4: "In an accompanying paper. . ." In my understanding, we will need results of Song et al. (2015) to infer $dH/d\lambda$ from satellite radiance measurements. Once we get $dH/d\lambda$ from the satellite measurements (or slope), we can estimate H from the parameterization equation in this manuscript. I think this discussion is more relevant when authors explain possible application, e.g. Section 9. It does not carry practical knowledge to readers in Introduction stage.

Thank you for catching this; we deleted the radiance-related statement here. The shortened paragraph now reads as follows:

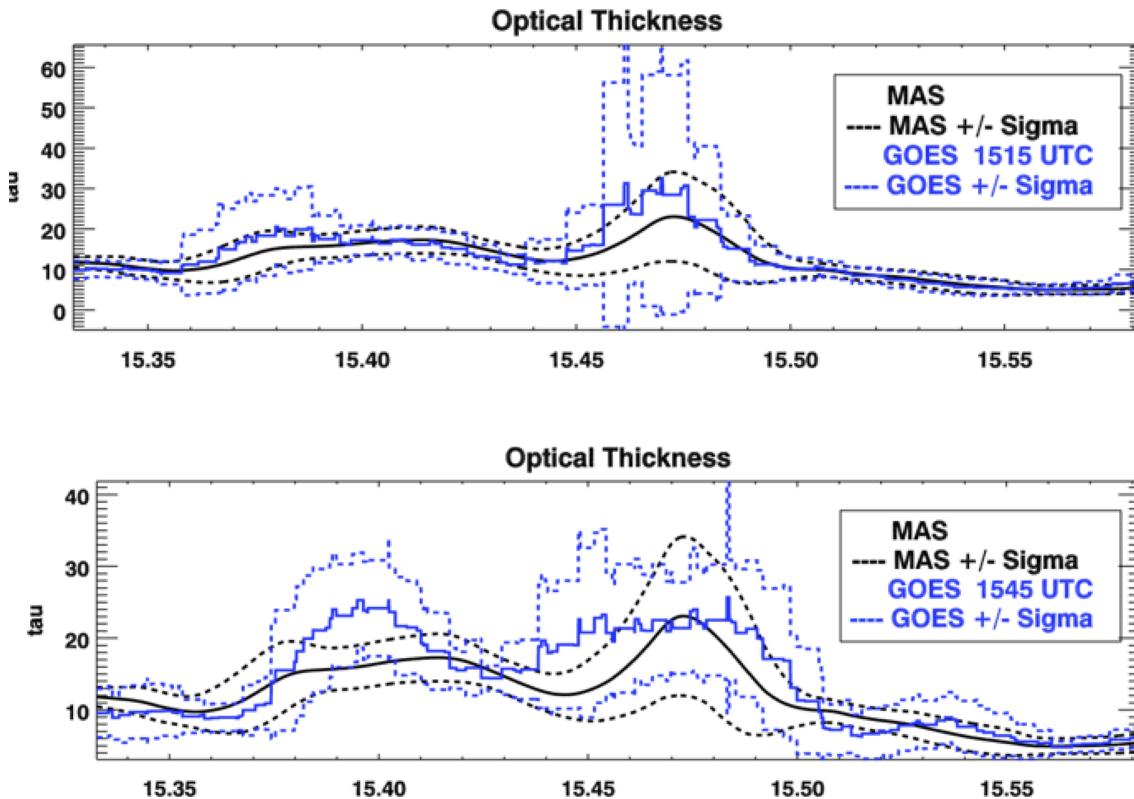
"Further analysis of the relationship between cloud structure and its spectral signature, presented here, revealed a surprisingly robust correlation between the magnitude of H and its spectral slope, $dH/d\lambda$. In the course of this paper, we provide evidence for molecular scattering as the physical mechanism behind this correlation and develop a simple parameterization based on this knowledge. We also examine at which spatial aggregation scale H can be ignored and whether the discovered correlation between H and $dH/d\lambda$ is scale invariant. Finally, we consider the ramifications of our findings on the shortwave surface energy budget and find that while cloud transmittance biases may be significant even after spatial averaging, they are also accompanied by spectral perturbations similar to the ones that we encountered for H . These biases may thus be detectable and correctable using adequate ground-based radiometers."

#6 Line 8, Page 8: "The spectral dependence of ..the full shortwave range" I think the authors cited Song et al. (2016) since this manuscript considered part of shortwave (< 1000 nm). Please state the wavelength range that this study covers.

The originally cited work (Song 2016, a dissertation, has now been published) actually changed scope and actually no longer covers any wavelengths beyond the near-UV, visible, and very near infrared. We have therefore removed this reference. We would like to point out here that there is work that has been done by Marshak and others for *radiances*, (Marshak, Evans, et al., 2014) and we added a statement to this effect. We also added a reference to Kassianov and Ovtchinnikov (2008).

#7 Line 1, Page 10: “we chose the earlier one because it was more consistent with the MAS retrieval” The 1515 UTC is more consistent with MAS in terms of cloud optical depth? Or perhaps 1515 UTC is closer to MAS observation time? Please clarify this.

This question allows us to show plots that we chose not to include in the manuscript. As the reviewer suggested, we used cloud optical depth to chose from two possible GOES scenes. The first plot shows the collocated MAS/GOES15:15 optical depth within 0.1° around the ER-2 latitude and longitude along the flight track. The second plot shows the same, but with the later GOES retrieval (15:45).



In terms of the timing, both GOES retrievals would be possible because the ER-2 flight leg (15:21-15:33) is right in between 15:15 and 15:45. However, the comparison of the MAS- and GOES retrieved optical thickness is more consistent when using the 15:15 scene. We changed the text as follows to make this clear: “In the sampling region, cloud property retrievals were produced at 15:15 and 15:45 UTC (Walther and Heidinger, 2012), of which we chose the earlier time because it was more consistent with the MAS retrieval in terms of the optical thickness along the ER-2 track.”

#8 Figure 2: From Figure 2, it seems that MAS domain is located boundary of cloud system, according to GOES retrieval. Figure 1 still shows large optical depth up to 80. How consistent MAS and GOES optical depths?

This observation is correct. The MAS swath does capture the edge of a cloud system (as shown in Figure 2). The color scale of Figures 1 and 2 is different; even GOES shows a

fairly large optical thickness on the NE edge of the MAS swath. Because of the different pixel size, GOES and MAS retrievals are not expected to match exactly. For this reason, the retrievals were aggregated to 0.1° “super-pixels” in the optical thickness plots above. The edge of the cloud system that the reviewer mentions is sampled at UTC=15.47 by the ER-2, and MAS and GOES show optical thickness values of ~20-30 at this aggregation scale. The higher optical thickness values as observed by MAS (~60) are small-scale maxima. In general, GOES and MAS retrievals are consistent within the range of the standard deviation in the 0.1° circle.

Note that the agreement in other retrieval parameters (cloud top height, effective radius) was not as good, in part because of different channel combinations that were used by the MAS / GOES algorithms. We chose not to go into detail about the MAS/GOES consistency in this paper because this is not its main purpose; such studies may be done in a separate paper.

#9 Line 16, Page 11: It would be helpful if the authors provide # of photons per pixel and corresponding accuracy (e.g. $1/\sqrt{N}$).

We included some more information on the photon number in the revised manuscript.

Small domain: $1e11$ or $7.4e6$ per pixel

Large domain: $1e12$ or $4.3e6$ per pixel

These photon numbers led to sufficiently low noise level. For example, the maximum standard deviation for the upwelling irradiance at the pixel level is $0.008 \text{ W/m}^2/\text{nm}$ at 500 nm.

#10 Line 3, Page 12: Is it true that H_0 cannot exceed 100%? H_0 is divergence of horizontal photon transport (e.g. Eq. A7 in Marshak et al. (1998)). Therefore, it should be rare, but isn't it theoretically possible that $H_0 > 100\%$?

Marshak et al. (1998) Biases in Shortwave Column Absorption in the Presence of Fractal Clouds, J CLI, 11, 431-446.

Thank you for this excellent catch! The reviewer is of course correct; this erroneous statement survived our internal review process. In fact, we found cases (in our own analysis for the next paper) where H_0 does exceed 100%. We simply deleted this statement, the revised version reads: “When H_0 falls below -100% , the radiation received through the sides of a column or voxel exceeds that from the top of the domain.” We don't state that the opposite is also true (for $H_0 > 100$, but that goes without saying).

#11 Line 3-4 page 13: molecular scattering as the underlying cause for this spectral dependence. This is a bit different from conclusion in Schmidt et al. (2010) (paragraph [33]). Could the authors explain the difference?

A very good point! We need to provide a little bit of background to explain this. The statement from Schmidt et al. (2010) in question is the following: “Preliminary tests showed that switching off molecular scattering in the RT model did not change the

slope significantly, thus ruling out molecular scattering as the cause for the spectral slope of the apparent absorptance.” In light of new evidence, the second part of this statement is, in fact, incorrect, but we must emphasize the word “preliminary”. It is true that when switching off molecular scattering, the slope did not change in this earlier study (incidentally done with a different model than used here). We therefore had to assume that the reason for the slope must lie elsewhere. At least two colleagues in the field thought that molecular scattering could not have such a large effect on irradiance (in contrast to radiance where it had been found at this point). While we always suspected molecular scattering, we could not present evidence at this point. In light of this, we should have worded this statement more cautiously. As it only turned out later, the explanation was that the switch in the model was actually inactive (keeping molecular scattering on regardless of the switch settings). We did not suspect this until after the paper was published, at which point we had a conversation with one of the code developers who brought up this possibility. In retrospect, this was a user error because we should have been able to diagnose this problem with further runs. We have since done these tests and found the cause of the problem. The analysis in the current paper (Figure 3) correctly shows that molecular scattering does explain the phenomenon. We added the following statement about the earlier study: “Note that the earlier study by Schmidt et al. (2010) remained inconclusive as to the mechanism of the spectral dependence they observed.” This is justified as the earlier study states (in the conclusions): “The physical basis of the spectral shape of near - UV and visible apparent absorption remains to be explored, as well as the scales over which horizontal photon transport occurs in high - cloud systems (for example, by embedding the MAS cloud scene in the larger context of GOES retrievals).”

#12 Line 14-18, Page 17: “In this context, it is. . .above a cloud field.” It is hard to understand this paragraph. Could the authors consider revise this paragraph? Also radiance in this paragraph means spectral radiance and irradiance is angle-integrated spectral radiance?

We simply deleted this paragraph because it distracted from the main content.

#13 Line 1, page 18: CERES algorithm converts broadband radiance into irradiance without taking into account 3D effects, even though the ADM is based on observation. For example, if the CERES observes radiance in illumination side, radiance for that angle is higher than other angles, but ADM does not consider this. Therefore, I guess the derived irradiance is not completely free from 3D errors. Of course these errors are negligible if we get enough samples and take average spatially and temporally.

We agree, and the Ham et al. (2014) publication (cited in our paper) talks about the effect of horizontal photon transport (not so much about illumination though). However, the 3D errors in transmitted irradiance should be much larger than in albedos because in principle, the ADMs do include spatially inhomogeneous conditions, however sparsely the parameter space may be sampled for those. Also, our statement was meant in the statistical sense, i.e., averaging over multiple

“realizations” of such scene types. We modified our statement as follows: “In principle, the mean albedo of an inhomogeneous cloud field derived from CERES observations should be fairly insensitive to 3D effects because they are statistically folded into anisotropy models of such scene types (if these empirical models adequately accomplish the radiance-to-irradiance conversion for a range of sun-sensor geometries).”

#14 Line 19-20, Page 20 I wonder why two equations in line 19-20 do not [have] absorption terms.

$$TIPA+RIPA+AIPA=1$$

$$T3D+R3D+A3D+H=1$$

Then Eq. (14) is $H=\Delta T+\Delta R + \Delta A$

This set of equations was written for conservative scattering (no absorption), but since the other reviewer also noted the lack of absorption, we made this more clear by slightly rewording as follows: “Juxtaposing energy conservation for a horizontally homogeneous atmosphere ($TIPA + RIPA = 1$) with Eq. (1) for conservative scattering ($A=0$, therefore $T3D + R3D = 1 - H$) yields the plausible relationship...”

#15 From Eq. (14), horizontal transport term H is partitioned into 3D effects on reflection, absorptance, and transmittance (ΔT , ΔR , and ΔA). I think ΔT is strongly correlated with H since absolute magnitude of ΔT is the largest among ΔT , ΔR , and ΔA . Note that cloud albedo is 30%, atmosphere transmittance is 50%, and atmosphere absorption is 20%.

This is an interesting thought, and we believe that this partitioning may need to be investigated in the future. It is indeed plausible that the bias is correlated with the magnitude of T and R itself. However, we did not attempt to do the partitioning in the study and focused mainly on the transmittance in the remainder of the paper. We do note that H at the pixel level is correlated with ΔT , but not with ΔR . However, we do not draw conclusions about the magnitude of the two biases. Comparing Figure 9b with Figure 10 does show that the range of ΔT is larger than that of ΔR , however the point there is not the magnitude but the correlation with H. As to Figure 10, it was surprising to us that R and H do become correlated at scales greater than 5 kilometers.

#16 The authors noted that 3D effects are significant even for large scale. However, previous studies already showed that instantaneous 3D effects might be large, but domain-averaged 3D effects are small. I think the authors need to use ‘instantaneous’ term if necessary, to differentiate from domain-averaged 3D effects.

The emphasis of the paper as a whole was on the spectral aspect of this problem, not on the magnitude of the 3D effect, for which the single case presented in the paper

would not have sufficient statistics anyway. We confirm that we mean a *local* 3D effect, rather than the domain-average effect. We prefer “local” to “instantaneous” as suggested by the reviewer because it is tied to space rather than time. Where appropriate, we added “local” in the few occurrences where we do talk about magnitudes. For example, the section in the abstract reads as follows: “In the case we studied, neglecting net horizontal photon transport leads to a **local** transmittance bias of ± 12 -19% even at the relatively coarse spatial resolution of 20 kilometers.” More changes have been made to section 7. In other cases, we made clear that we are talking about pixel-level effects and biases. We agree that in the domain average (as shown in previous papers), 3D biases become small. At the same time though, our study showed that even aggregating the data to large scales, significant biases survive. Figure 8d is meant to illustrate this. One can essentially read off the biases for various aggregation scales. For example, at 0.5 km pixel size, we get >50% biases. Averaging to 20 km decreases the bias to just over 10%, and it eventually disappears at even larger aggregation scales. We do believe that Figure 8d and the text accompanying makes this clear. We fully agree with the comment by the reviewer and do not contradict earlier studies.

More recent research (Song, 2016) shows that by considering 3D effect on irradiance (as done in this paper) *and* on cloud remote sensing may lead to biases in transmitted irradiance estimates that do not disappear with increasing scale but survive averaging. This research will also be presented in a separate paper (Song et al., 2016).

Response to review of “The spectral signature of cloud spatial structure in shortwave irradiance” by anonymous Referee #2

Sebastian Schmidt, corresponding author

We thank the reviewer for the positive assessment of the manuscript and the helpful comments regarding the clarity and cohesion. We shortened the introduction, leaving out unnecessary references to the radiance aspect of the problem, which helped the cohesion of the manuscript. Owing to the reviewer’s positive feedback, we kept the conclusion section largely unchanged. Regarding the applicability of our parameterization, see our response to general comment #2. [Note that page/line numbers refer to the original, not the revised manuscript.]

Assessment: Minor Revisions

General comments:

#1 There are several places in the manuscript related to radiances instead of irradiances (e.g., p17, 111ff) . For the flow of the paper discussions concerning the relation between H and radiance measurements by satellites should be shifted to the end of the paper.

This is an excellent point; the other reviewer had a similar comment. The discussion of radiances interrupted the flow of the paper; we removed multiple occurrences in the body of the paper and discussed it mainly in the conclusions. Rather than going into too much detail in this paper, we instead included a reference to a Ph.D. and the companion paper (Song et al. 2016, to be submitted soon). Changes are highlighted in the revised version of this paper.

References:

Song, 2016: The Spectral Signature of Cloud Spatial Structure in Shortwave Radiation, *Ph.D. thesis, University of Colorado at Boulder*.

Song, S., K. S. Schmidt, Pilewskie, P., King, M. D., Platnick, S., 2016: Quantifying the spectral signature of heterogeneous clouds in shortwave radiance and irradiance measurements, to be submitted to *JGR SEAC⁴RS special issue*

#2 It is not completely clear how to use your findings for other users. How can we improve for example layer properties calculations from airborne irradiance measurements with respect to horizontal photon transport?

The other reviewer also brought up this point. Indeed, the term “parameterization” might suggest that it can be exploited for inferring, simplifying, or correcting 3D effects, and the authors are currently working on this topic. However, the parameterization is only the first step towards this goal, and it cannot (yet) be translated into such immediate practical applications, although this is certainly the goal for the future. The purpose of the parameterization is to capture the relationship between net horizontal photon transport

and its spectral dependence using one main parameter (ϵ). The companion paper (Song et al., 2016) will look at the connections between 3D effects on irradiances and radiances. We will include this explanation in the revised version. For example, we conclude the abstract with the following statement: “Since three-dimensional effects depend on the spatial context of a given pixel in a non-trivial way, the spectral dimension of this problem may emerge as the starting point for future bias corrections.” In section 6, we included this statement “Although our study was instigated by aircraft measurements, its findings are also relevant for satellite-based derivations of cloud radiative effects since the spectral perturbations $d\lambda$ propagate into observed radiances (Song et al., 2016). This may be exploited in future applications for deriving correction terms for 3D radiative effects via their spectral signature.” We hope this clarifies the purpose of the parameterization.

Specific comments:

#1 In the last sentence of the abstract the authors mention a companion paper. It is not necessary to refer to this publication in the abstract. Rather the authors should give an example how and where the parameterization can be applied for other users.

We made this change. We also added an outlook as final sentence in the abstract, which makes clear how the correlations and the parameterization may be used in the future (“Since three-dimensional effects depend on the spatial context of a given pixel in a non-trivial way, the spectral dimension of this problem may emerge as the starting point for future bias corrections.”) At this point, the parameterization is useful to understand measurements of horizontal photon transport in inhomogeneous scenes, and can essentially be used as “fitting function” for the spectra with the free parameter ϵ . We will include a statement to this effect in the next paper (Song et al., 2016). In fact, this has already been done in the Ph.D. thesis (Song, 2016) which will become available for download on 8/18/2016. Once this happens, we will include a link and reference in this paper.

#2 (p3, 17) “can assume similar values as the absorbed irradiance”; Comparing the apparent absorption shown in Fig. 4a (500 nm) and 4b (1600 nm) in Schmidt et al. (2010) I identify the more the same magnitude than similar values. It’s still a variable factor between the numbers. Use “same magnitude” instead “similar values”. In addition, the authors should give reasons for smaller H-values in the NIR.

We changed the wording slightly to make this distinction. We actually did not say that H values are smaller in the NIR; we only compared H (VIS) to A (NIR). A more thorough discussion is given by Schmidt et al. (2010).

#3 (p3, 120ff) The wavelength dependence of horizontal photon transport is mentioned here. Could you give a more detailed literature review on this since it is crucial for the entire manuscript?

There have been many studies on the wavelength dependence of 3D effects in *radiance*, and the manuscript cites a small sub-set of these in Section 5 (Wen et al., 2007; Marshak et al., 2008; Varnai and Marshak, 2009), at which point the connection to the irradiances

is made. It reads as follows: “Remote sensing studies (e.g., Marshak et al., 2008; Várnai and Marshak, 2009) had previously established that the above-mentioned *radiance enhancement* for clear-sky pixels near clouds was associated with “apparent bluing,” and proposed molecular scattering as the underlying cause for this spectral dependence.” Following the reviewer’s suggestion, we did add two additional studies pertaining to radiances (Marshak et al., 2014; Kassianov and Ovtchinnikov, 2008) further up in the text, which now reads: “For the extreme case of zero cloud optical thickness, the effect of horizontal photon transport had previously been observed as clear-sky radiance enhancement in the vicinity of clouds (Wen et al., 2007; Kassianov and Ovtchinnikov, 2008; Várnai and Marshak, 2009; Marshak et al., 2014).”

Unfortunately, studies for *irradiances* are rare, and the only ones that the authors were aware of (Ackerman and Cox, 1981; Marshak et al. 1999; Kindel et al., 2011) had been cited. However, the most relevant study (the one by Kassianov) had only been included as a footnote, and we moved it into the body of the text at the location commented on by the reviewer.

#4 (p4, 12-15) The paragraph is a mixture of outline and outlook (16-9). Please strengthen the content. A structure of the paper is already described in the last paragraph of the introduction. Therefore the idea of the paper should be presented before (performing 3D and 1D simulations with a measured cloud data set, identifying H and it’s spectral behavior, . . .) without prejudging the results.

Thank you for catching this, we agree. We deleted the lines in question (L6-9, also 13-15). We also shortened the introduction in general.

#5 (p5, 118) Eq. (3) states the spectral absorptance. Add here directly, that these layer properties are valid for homogeneous conditions without horizontal photon transport. The reader might be confused otherwise because Eq. (3) contradicts Eq. (1) without this restriction (as noted only on p.6, 15-7).

Thank you for this helpful comment. We made the reader aware of the difference between (1) and (3) by pre-ambling the formula with this statement: “For **homogeneous conditions ($H=0$)**, this can be quantified in terms of the layer property absorptance”.

#6 (p8, 18-12) This paragraph gives an outlook. Better put this at the end of the manuscript.

This statement (18-12) was deleted.

#7 (p9, 14-6) As stated by the authors using height-constant effective radii has an effect on the vertical distribution of the phase functions which probably differ from reality. Why does the phase function don’t affect the 3D radiative transfer? Changes of the phase function result in changes of the scattering direction. Maybe this is not as relevant as for radiance simulations. Please clarify.

We agree that this simplification undoubtedly has an effect, and we only made this

simplification lacking better data. It is true that this would be a bigger problem for radiances than for irradiances because of the hemispherical integration. Luckily, this paper is basically a *modeling* study, albeit based on observations. We preferred actual imagery data to idealized cloud fields, which arguably could also have worked to carry out the study. Whether or not our calculations actually depicted the truth is therefore not as relevant for the message of the paper. This is different in the follow-on study (Song et al., 2016) where we used actual irradiance measurements to validate the model output.

#8 (p9, 18) Please define WC.

Done (it's water content, not a sanitary facility ☺).

#9 (p9, 117) Please justify the choice of spatial resolution (with respect to typical spatial scales of radiative smoothing).

The chosen resolution is certainly not fine enough to reproduce radiative smoothing in the radiance fields, but that was also not the point of the paper, which focuses on radiative energy budget quantities instead. The finest scale that is usually considered in such studies is 1km. We modified the sentence in question to “The resulting cloud field was gridded to a resolution of 0.5 km horizontally (**similar to the MODIS pixel size of some channels**) and 1.0 km vertically (chosen larger than the mismatch between CRS and MAS in cloud top height),” in order to convey our motivation for 0.5 km as spatial resolution. Undoubtedly, a finer resolution would be better, but it would have been computationally prohibitive to achieve appropriate signal-to-noise level for each of the pixels.

#10 (p11, 116) What will be generalized? The solar position?

We modified the sentence as follows: “The scene parameters (solar geometry, surface albedo, cloud properties) will be generalized in future work (Song, 2016).”

#11 (p12, 18-11) The enhancement of radiance in the vicinity of clouds is mentioned here. Can you cite also papers dealing with the enhancement of irradiances? Add also the fact that this effect is wavelength-dependent.

We added more references at this point (Wen et al., 2007; Kassianov and Ovtchinnikov, 2008; Várnai and Marshak, 2009; Marshak et al., 2014). See also our response for comment #3 regarding the wavelength dependence. We did not really mention the enhancement of *irradiances* in this context; this has been done in numerous other studies (including two of our own, Schmidt et al., 2007; 2009). We didn't cite these here because we wanted to keep this focused at the wavelength dependence. Note that the Kassianov paper is the only one (to our knowledge) besides the Ackerman and Cox paper which addresses this topic.

#12 (p13, 115) Could you insert the linear fit in Fig. 3a?

Done, and we added a statement later on (following the discussion of Equation (12)) that a linear fit is less accurate than the spectrally dependent parameterization that we

developed later on: “This is more accurate than the derivation of the slope from a linear fit to the spectrum as used for Fig. 3, which, due to the non-linearity of the spectral dependence, differs from that of the tangent if finite wavelength intervals are used.”

#13 (p13, l24) “pixel-to-pixel radiation exchange” → Please add “horizontal” here. There is of course a vertical exchange of photons.

Done.

#14 (p18, l16-19) “Eq. (1) suggests...” In my opinion these two sentences do not contribute significantly to the context of this section. Referring to transmittance here somehow interrupts the flow of the discussion on spatial aggregation.

We deleted these two sentences.

#15 (p20, l20) Please motivate the restriction of conservative scattering here, otherwise the missing absorption term might confuse the reader.

We did remind the reader in a few places that we are only talking about wavelengths where clouds do not absorb; the general equations including A are only used to motivate our study in the introduction. However, the other reviewer also commented on the potential confusion on p20/L20, and to make it clear that we are making the simplification of $A=0$, we modified the text as follows: “Juxtaposing energy conservation for a horizontally homogeneous atmosphere ($TIPA + RIPA = 1$) with Eq. (1) for conservative scattering ($A=0$, **therefore** $T3D + R3D = 1 - H$) yields the plausible relationship...” We will turn our attention to wavelengths where clouds do absorb in a future study.

#16 (Sect. 8, first paragraph) To make sure that the equations are valid only for a specific wavelength range, the index “ λ ” would be helpful for H , R , T ,...

We preceded the formulae with this statement “For any atmospheric column, H is connected to R and T through Eq. (1) and manifests itself in a transmittance and reflectance bias (λ index omitted):” to indicate that the following discussion addresses a range of wavelengths (with conservative scattering, as later explained).

#17 (p23, l4, l10) If you give numbers here then you have to mention that these numbers are case specific with respect to surface albedo and solar position.

We modified the text as follows to clarify the scene dependence of ε : “ $\varepsilon = 0.7 \pm 0.1$ **for the scene we studied**” on p23,l10. As for the x parameter, it is not scene dependent. We did not make a strong statement about this in this manuscript because more scenes will need to be studied, but it is plausible that $x \sim 4$ would not change much from scene to scene, whereas ε depends on scene parameters such as surface albedo. We pointed out the need for further studies on what drives ε in the following question (conclusions): “How does the discovered correlation and the constant of proportionality in its parameterization,

ε , depend on scene parameters such as solar zenith and azimuth angle, surface albedo (magnitude and spectral dependence), and cloud morphology and microphysics? What “drives” the parameter ε ?” This question is addressed by Song (2016, chapter 4), and the content of this dissertation chapter will likely be published as a stand-alone paper at a later time (probably combined with the generalization to NIR wavelengths).

#18 (Sect. 9) Be more consistent with using indices for H. For example p.23, l.16: Is it H or H_0 or H_λ which has to be known?

We attempted to follow this suggestion and went through the indexing in the manuscript. In this particular place, we changed as follows: “Once ε is established for a given cloud scene, the spectral perturbations associated with horizontal photon transport can be derived for each pixel if the value of H_0 is known. Conversely, if the spectral shape of H_λ is known at one wavelength, its magnitude can easily be inferred for the whole spectrum.”

#19 (Fig3b) Is there any reason for the increasing scatter[ing] of 3D-based S_0 – H_0 correlation for negative slopes?

Great question; there are two parts to this: (a) the asymmetry between the (negative) minimum of H_0 and the (positive) maximum [probably not what the reviewer referred to] and (b) the increasing variability of S_0 for a fixed (negative) H_0 .

Regarding (a): In the domain average, $\langle H_0 \rangle = 0$ despite the asymmetry. This is because fewer cloudy pixels with high values of H_0 balance a larger number of clear or low-optical thickness pixels with smaller (negative) values of H_0 .

Regarding (b): We don’t have a very good understanding of this yet, but the likely explanation is that for pixels that are clear or have low optical thickness, the spectral signature associated with horizontal photon transport may be affected by additional processes that are not captured by the simplified mechanism as presented in Figure 5. For example, for an optical thickness < 4 , the partial compensation to horizontal photon transport through molecular scattering as indicated by blue arrows may become more complicated. We did not comment on this extensively and leave this to the future. We did, however, add the following statement to section 6: “Note that below $\tau \approx 4$, directly transmitted radiation dominates the downwelling irradiance, and the cloud may not act as a “diffuser” as shown in Fig. 5. The direction of the green arrows is then along the direct beam.” This effect is most likely the cause for the deviation from the correlation that the reviewer observed.

Technical comments:

1) Please remove footnotes

Done.

2) Check that symbols in figures have italic format.

Done, figures were replaced.

3) (p12, 125) Figs. → Fig. 4): (p13, 125) “H” → “H₀” 5): (p14, 13) “H_λ” → “H_λ” (italic)

All done, thanks.

Style Definition: Reference: Left

1 The spectral signature of cloud spatial structure in shortwave 2 irradiance

3 Shi Song^{1,2}, K. Sebastian Schmidt^{1,2}, Peter Pilewskie^{1,2}, Michael D. King², Andrew K.
4 Heidinger³, Andi Walther³, Hironobu Iwabuchi⁴, Gala Wind⁵, Odele M. Coddington²

Formatted: Superscript

5 [1] Department of Atmospheric and Oceanic Sciences, University of Colorado, Boulder, CO,
6 USA

7 [2] Laboratory for Atmospheric and Space Physics, University of Colorado, Boulder, CO, USA

8 [3] NOAA Center for Satellite Applications and Research, Madison, WI, USA

9 [4] Center for Atmospheric and Oceanic Studies, Tohoku University, Japan

10 [5] Space Systems and Applications, INC., Greenbelt, MD, USA

13 Abstract

14 In this paper, we used cloud imagery from a NASA field experiment in conjunction with three-
15 dimensional radiative transfer calculations to show that cloud spatial structure manifests itself as
16 spectral signature in shortwave irradiance fields – specifically in transmittance and net horizontal
17 photon transport in the visible and near-ultraviolet wavelength range. We found a robust
18 correlation between the magnitude of net horizontal photon transport (H) and its spectral
19 dependence (slope). which is scale-invariant and holds for the entire pixel population of a
20 domain. This was at first surprising given the large degree of spatial inhomogeneity. We prove
21 that the underlying physical mechanism for this phenomenon is molecular scattering in
22 conjunction with cloud spatial structure. On this basis, we developed a simple parameterization
23 through a single parameter ϵ , which quantifies the characteristic spectral signature of spatial
24 inhomogeneities. In the case we studied, neglecting net horizontal photon transport leads to a
25 local transmittance bias of $\pm 12-19\%$ even at the relatively coarse spatial resolution of 20
26 kilometers. Since three-dimensional effects depend on the spatial context of a given pixel in a

Deleted: We found that c

Deleted: In this paper, we demonstrate this through radiative transfer calculations with cloud imagery from a field experiment, and show that such three-dimensional effects may occur on scales up to 60 kilometers. Neglecting net horizontal photon transport leads to a transmittance bias on the order of $\pm 12-19\%$ even at the relatively coarse spatial resolution of 20 kilometers, and of more than $\pm 50\%$ for 1 kilometer. This poses a problem for radiative energy budget estimates from space because the bias for any pixel depends on its spatial context in a non-trivial way. The key for solving this problem may lie in the spectral dimension, since w

Deleted: . It

Deleted: , but seems to be valid for any cloud field

Deleted: inhomogeneity

Deleted: heterogeneities

1 non-trivial way, the spectral dimension of this problem may emerge as the starting point for
2 future bias corrections.

Deleted: In a companion paper, we will show that it is accompanied by spectral radiance perturbations, which can be detected from multi-spectral imagers and may be translated into bias reductions for cloud radiative effect estimates in the future.

4 1. Introduction

5 Determining cloud radiative effects for scenes with a high degree of spatial complexity
6 remains one of the most persistent problems in atmospheric radiation, especially at the surface
7 where satellite observations can only be used indirectly to infer energy budget terms. In the
8 shortwave (solar) spectral range, it is especially challenging to derive consistent albedo,
9 absorption, and transmittance from spaceborne, aircraft, and ground-based observations for
10 inhomogeneous cloud conditions (Kato et al., 2013; Ham et al., 2014). This problem is closely
11 related to the long-debated discrepancy between observed and modeled cloud absorption
12 (Stephens et al., 1990) since energy conservation for a three-dimensional (3D) atmosphere
13 (Marshak and Davis, 2005, Eq. 12.13)

$$14 \quad R + T = 1 - (A + H) \quad (1)$$

Formatted: Font:Italic

15 connects reflectance R , transmittance T , and absorptance A of a layer. The term H accounts for
16 lateral net radiative flux from pixel to pixel (which we will call net horizontal photon transport).

Deleted: ¹

17 Out of necessity, most algorithms for deriving R , T , and A from passive imagery inherently
18 presume isolated pixels by relying on one-dimensional (1D) radiative transfer (independent pixel
19 approximation) which does not reproduce H . Net horizontal photon transport has therefore long
20 been a common explanation not only for inconsistencies between measured and calculated
21 broadband cloud absorption (Fritz and MacDonald, 1951; Ackerman and Cox, 1981) but also for
22 remote sensing artifacts (Platnick, 2001).

Deleted: ²

23 Observational evidence for this explanation emerged with the availability of spectrally
24 resolved aircraft measurements of shortwave irradiance (Solar Spectral Flux Radiometer, SSFR:
25 Pilewskie et al., 2003). Schmidt et al. (2010) derived *apparent absorption*, the sum of A and H ,
26 from irradiance measurements aboard the NASA ER-2 and DC-8 aircraft that flew along a
27 collocated path above and below a heterogeneous anvil cloud during the Tropical Composition,

1 Cloud and Climate Coupling Experiment (TC⁴) (Toon et al., 2010). ~~The results of this study~~
2 ~~showed that, in~~ absolute terms, H at visible wavelengths (where cloud and gas absorption are
3 negligible) can ~~attain a similar magnitude~~ as the absorbed irradiance A at near-infrared
4 wavelengths. Horizontal photon transport thus has the potential to mimic substantially enhanced
5 absorption. Three-dimensional (3D) calculations confirmed the measurements, and radiative
6 closure was achieved within measurement and model uncertainties without invoking proposed
7 enhanced gas absorption (Arking, 1999) or big cloud droplets (Wiscombe et al., 1984). The
8 results also suggested that the overestimation of absorption would persist even when averaging
9 over long distances as proposed by Titov (1998). This is simply because radiation flight legs are
10 often preferentially targeted at cloudy regions ($\langle H \rangle > 0$) and do not adequately sample clear-sky
11 areas where photons are depleted ($\langle H \rangle < 0$), which is interpreted as *apparent emission* in
12 measurements.

13 Perhaps the most significant finding by Schmidt et al. (2010) was the distinct spectral
14 shape of H from the near-ultraviolet well into the visible wavelength range, leading to the notion
15 of “colored” net horizontal photon transport (Schmidt et al., 2014). ~~A previous study addressing~~
16 ~~horizontal photon transport from an energy budget point of view (Kassianov and Kogan, 2002)~~
17 ~~had focused on the wavelength range of 0.7-2.7 μm , specifically to avoid molecular scattering at~~
18 ~~shorter wavelengths.~~ Strategies for mitigating the overestimation of cloud absorption (Ackerman
19 and Cox, 1981; Marshak et al., 1999) require that H be more or less constant in the visible
20 wavelength range (Welch et al., 1980), and so the discovery of the spectral dependence of H
21 suggested that they should be applied with caution. ~~For example, Marshak et al. (1999) in their~~
22 ~~conditional sampling technique required that $H = 0$ for at least two~~ *different wavelengths*. Kindel
23 ~~et al. (2011) applied such a modified scheme for boundary layer clouds.~~

24 Further analysis of the relationship between cloud structure and its spectral signature,
25 presented here, revealed a surprisingly robust correlation between the *magnitude* of H and its
26 *spectral slope*, $dH/d\lambda$. In the course of this paper, we provide evidence for molecular scattering as
27 the physical mechanism behind this correlation and develop a simple parameterization based on
28 this knowledge. ~~We also~~ ~~examined~~ at which spatial aggregation *scale* H can be ignored and

Deleted: The spectral dependence of apparent absorption as well as its pixel-to-pixel variability showed that in

Deleted: assume similar values

Deleted: (where $|H| \ll A$)

Deleted: in broadband measurements

Deleted: ³

Deleted: ⁴

Formatted: Font:Italic

Deleted: In an accompanying paper (Song et al., 2015), we will demonstrate that cloud spatial inhomogeneities also manifest themselves in spectral *radiance* perturbations via $dH/d\lambda$, which can be used for deriving H correction terms for cloud radiative effects of inhomogeneous scenes from space-borne observations.

Deleted: We

Deleted: complete our paper by

Deleted: ing

1 whether the discovered correlation between H and $dH/d\lambda$ is scale invariant. Finally, we
2 considered the ramifications of our findings on the shortwave surface energy budget.

Formatted: Not Highlight

Deleted: and find that while cloud transmittance biases may be significant even after spatial averaging, they are also accompanied by spectral perturbations similar to the ones we encountered for H . These biases may thus be detectable and correctable using adequate ground-based radiometers.

3 Following this introduction, we provide definitions of relevant terms and explain how H
4 relates to top-of-atmosphere (TOA) and surface cloud radiative effects (CRE). We then discuss
5 the data and model calculations that lay the basis for our study (Sections 3 and 4). In section 5,
6 we discuss the correlations between H and $dH/d\lambda$, followed by the underlying physical
7 mechanism and parameterization presented in Section 6. The discovered relationship is then
8 examined as a function of spatial scale (Section 7) and interpreted in terms of the surface CRE
9 (Section 8). In the conclusions, we discuss the significance of our findings and propose multi-
10 spectral or spectral techniques for deriving first-order correction factors in CRE estimates from
11 space, aircraft, and from the surface that may render 3D calculations unnecessary.

12 2. Net horizontal photon transport and cloud radiative effect

13 The instantaneous radiative effect of any atmospheric constituent is the difference of net
14 irradiance (flux density) in its presence (all-sky) and absence (clear-sky). For clouds, we define

$$15 \quad CRE_{\lambda} = \left[\frac{(F_{\lambda}^{\downarrow} - F_{\lambda}^{\uparrow})_{all-sky}}{F_{\lambda}^{\downarrow,TOA}} - \frac{(F_{\lambda}^{\downarrow} - F_{\lambda}^{\uparrow})_{clear-sky}}{F_{\lambda}^{\downarrow,TOA}} \right] \times 100\%, \quad (2)$$

16 where F_{λ}^{\downarrow} and F_{λ}^{\uparrow} are downwelling and upwelling irradiance and their difference is net irradiance.
17 For this paper, we normalize the *absolute* radiative effect by the TOA downwelling irradiance
18 ($F_{\lambda}^{\downarrow,TOA}$) and consider the *relative* radiative effect as percentage of the incident irradiance. Also,
19 we use spectrally resolved rather than broadband quantities, indicated by subscript λ .

20 The TOA shortwave CRE is always negative (*cooling* effect) because the reflected
21 irradiance $F_{\lambda}^{\uparrow,TOA}$ in presence of clouds is larger than for clear-sky conditions. The surface
22 shortwave CRE is also negative because clouds decrease the transmitted irradiance $F_{\lambda}^{\downarrow,SUR}$, at
23 least for homogeneous conditions; broken clouds can locally increase surface insolation. In
24 contrast to the shortwave CRE at TOA and at the surface, homogeneous clouds have a *warming*
25 effect on the layer in which they reside. For homogeneous conditions ($H=0$), this can be
26 quantified in terms of the layer property absorptance

Deleted: T

Formatted: Font:Italic

$$A_\lambda = \left[\frac{F_\lambda^{\downarrow,top} - F_\lambda^{\uparrow,top}}{F_\lambda^{\downarrow,top}} - \frac{F_\lambda^{\downarrow,base} - F_\lambda^{\uparrow,base}}{F_\lambda^{\downarrow,top}} \right] \times 100\% \quad (3)$$

for a cloud located between h_{top} and h_{base} with the same normalization as used above for the relative CRE. It can be determined from aircraft measurements by collocated legs above and below the cloud (Schmidt et al., 2010). The warming within the layer arises from absorption ($A > 0$) primarily in the near-infrared wavelength range ($1 \mu\text{m} < \lambda < 4 \mu\text{m}$). Similarly, layer transmittance and reflectance are defined as

$$T_\lambda = \left(\frac{F_\lambda^{\downarrow,base}}{F_\lambda^{\downarrow,top}} \right) \times 100\% \quad (4)$$

$$\text{and } R_\lambda = \left(\frac{F_\lambda^{\uparrow,top} - F_\lambda^{\uparrow,base}}{F_\lambda^{\downarrow,top}} \right) \times 100\% . \quad (5)$$

Related to layer reflectance is the albedo $\alpha_\lambda = F_\lambda^{\uparrow} / F_\lambda^{\downarrow}$ (identical to R_λ for zero surface albedo). The sum of layer absorptance, transmittance, and reflectance defined in this way is 100% and thus satisfies energy conservation for horizontally homogeneous layers. For individual pixel sub-volumes within an inhomogeneous layer (voxels), A_λ in Eq. (3) can be replaced with $A_\lambda + H_\lambda \equiv V_\lambda$ where V_λ stands for the vertical flux divergence (the net irradiance difference above and below a layer). In this way, energy conservation including horizontal transport [Eq. (1)] is retained.

The difference of the CRE at TOA and at the surface from Eq. (2) can be related to Eq. (3) as follows:

$$CRE^{TOA} - CRE^{surface} = \left[\frac{(F_\lambda^{net,cloud} - F_\lambda^{net,clear})^{TOA}}{F_\lambda^{\downarrow,TOA}} - \frac{(F_\lambda^{net,cloud} - F_\lambda^{net,clear})^{surface}}{F_\lambda^{\downarrow,TOA}} \right] \times 100\% \quad (6a)$$

$$= \left[\frac{(F_\lambda^{net,TOA} - F_\lambda^{net,surface})^{cloud}}{F_\lambda^{\downarrow,TOA}} - \frac{(F_\lambda^{net,TOA} - F_\lambda^{net,surface})^{clear}}{F_\lambda^{\downarrow,TOA}} \right] \times 100\% \quad (6b)$$

The first term inside the brackets of Eq. (6b) is identical to A_λ from Eq. (3) if the boundaries of the layer h_{top} and h_{base} are extended to the TOA and surface, respectively. We denote this by \hat{A}_λ

Deleted: , as absorptance,

1 | and distinguish full-column properties using a **caret** (\hat{A} , \hat{H} , \hat{R} , \hat{T}) from the layer properties that
 2 | bracket only the cloud itself (A , H , R , T). The second term in Eq. (6b) stems from “clear-sky”
 3 | absorption by atmospheric constituents other than clouds (gases and aerosols). Eq. (6b) can then
 4 | be re-written as

$$\hat{A}_\lambda = CRE^{TOA} - CRE^{surface} + \left[\frac{(F_\lambda^{net,TOA} - F_\lambda^{net,surface})^{clear}}{F_\lambda^{A,TOA}} \right] \times 100\% \quad (6c)$$

6 | which simply means that the total atmospheric column absorption comprises contributions from
 7 | the cloud itself as well as from clear-sky absorption. In presence of horizontal inhomogeneities,
 8 | the left and right side of Eq. (6c) may be inconsistent unless \hat{A}_λ is replaced with $\hat{V}_\lambda = \hat{A}_\lambda + \hat{H}_\lambda$ as
 9 | above.

10 | Presented in this way, the central role of absorptance and horizontal transport in linking
 11 | the net irradiances above and below a cloud [Eq. (3)], as well as the TOA and surface CRE [Eq.
 12 | (6c)], becomes clear. While the global TOA CRE can directly be derived from reflected radiances
 13 | (Loeb et al., 2005), for example from the Clouds and the Earth’s Radiant Energy System
 14 | (CERES) on the Aqua and Terra satellites (Wielicki et al., 1996), the derivation of the surface
 15 | CRE also requires the knowledge of atmospheric absorptance or transmittance. In the case of
 16 | CERES, the required cloud properties are obtained from retrievals of the accompanying imager,
 17 | the Moderate Resolution Imaging Spectroradiometer (MODIS) (Minnis et al., 2011). As stated in
 18 | the previous section, this is accomplished through lookup tables which are based on 1D
 19 | calculations and therefore do not provide H .

20 | Recognizing the crucial significance of horizontal photon transport for obtaining an
 21 | accurate surface CRE, Barker et al. (2012) and Illingworth et al. (2015) described the ambitious
 22 | goal of using 3D radiative transport operationally in the European radiative budget experiment
 23 | Earth Clouds, Aerosols and Radiation Explorer (EarthCARE). They tested their algorithm with
 24 | A-Train data. As a metric for 3D effects, they employed the commonly used difference between
 25 | 3D and IPA calculations (e.g., Scheirer and Macke, 2003). In a similar manner, Ham et al. (2014)
 26 | calculated the effect of horizontal photon transport on cloud absorption, transmission, and

Deleted: hat

Deleted: ⁵

1 reflected radiance. They found these three quantities to be correlated when stratifying their results
2 by cloud type after spatial aggregation to at least 5 km.

3 Since the studies cited above pertained to EarthCARE and CERES, they only considered
4 broadband effects. This does not allow distinguishing between A_λ and H_λ by means of their
5 distinct spectral characteristics. Our approach, first presented by Schmidt et al. (2014), bridges
6 this gap. In this paper, we focus exclusively on the near-ultraviolet and visible wavelength range
7 and explore the spectral fingerprint from cloud inhomogeneities in conjunction with molecular
8 scattering in H_λ , which also imprints itself on reflected radiances (Song 2016; Song et al., 2016).
9 We chose not to include aerosols in either study, primarily to isolate the spectral signature of
10 heterogeneous clouds before considering the more general case of clouds and aerosols in
11 combination.

Deleted: will

Deleted: et al.,

Deleted: 5

Deleted: to

Deleted: .

... [1]

12 3. Cloud Data

13 Our study builds upon the results by Schmidt et al. (2010) and therefore uses the same
14 cloud case, a tropical convective core with anvil outflow, observed during the TC⁴ experiment on
15 17 July 2007 (from 1519 to 1535 UTC) by the NASA ER-2 aircraft about 300 km south of
16 Panama. Two realizations of the observed cloud field were used as input to 3D radiative transfer
17 calculations, one based on airborne imagery only (as in the earlier study, Section 3.1), and one
18 based on merged airborne and geostationary imagery (Section 3.2) to study large-scale effects.

19 3.1 Sub-scene from ER-2 passive and active remote sensors

20 Level-2 cloud retrievals of the Moderate Resolution Imaging Spectrometer (MODIS)
21 Airborne Simulator (MAS; King et al., 1996; King et al., 2010) were combined with reflectivity
22 profiles from the Cloud Radar System (CRS; Li et al., 2004) as described in detail by Schmidt et
23 al. (2010). The primary information originates from MAS optical thickness, thermodynamic
24 phase, effective radius, and cloud top height retrievals for each pixel (x,y) within the imager's
25 swath (roughly 20 km for a cloud top height of 10 km). The imagery-derived information was
26 extended into the vertical dimension z by simple approximations:

27 (1) The effective radius from MAS, $r_e(x,y)$, was used throughout the vertical dimension z

1 although representative only of the topmost layer. Since the study is limited to the near-
2 ultraviolet and visible wavelength range where cloud absorption is negligible, this
3 simplification only affects the scattering phase function. Approximating it with that at
4 cloud top is acceptable because to first approximation, 3D radiative transfer is determined
5 by the distribution of cloud extinction.

6 (2) The MAS-retrieved optical thickness $\tau(x,y)$ for each pixel was vertically distributed by
7 using the water content (WC) profile from CRS: $WC(z) = 0.137 \times Z^{0.64}$ (Liu and
8 Illingworth, 2000) where Z is the radar reflectivity from CRS in dBZ. Since $WC(z)$ is only
9 available along the flight track, nadir-only CRS profiles were also used across the entire
10 MAS swath (shifted vertically by z_0 to match the MAS cloud top height at off-nadir
11 pixels). Cloud extinction β for each voxel (x,y,z) was thus obtained as

$$\beta(x,y,z) = \tau_{MAS}(x,y) \times WC(z+z_0) / \sum_z WC(z)$$

13 Along the flight track, the mismatch between MAS- and CRS-retrieved cloud top height
14 is ≤ 0.5 km. The CRS-derived average cloud top height is 10.8 km, and the mean
15 geometrical thickness is 3.3 km.

16 The resulting cloud field was gridded to a resolution of 0.5 km horizontally (similar to the
17 MODIS pixel size of some channels) and 1.0 km vertically (chosen larger than the mismatch
18 between CRS and MAS in cloud top height).

19 Figure 1 shows the cloud optical thickness field from MAS after regridding, with the
20 nadir track highlighted as a dashed line. The length of this scene is 192 km (384 pixels in x), and
21 the width is 17.5 km (35 pixels in y).

22 3.2 Large-scale field from ER-2 data merged with geostationary imagery

23 To generalize our findings to larger scales than 17.5 km, we embedded the sub-scene from
24 the ER-2 remote sensors in the context of the large-scale cloud field as retrieved from the
25 Geostationary Operational Environmental Satellite West (GOES-11). The imager onboard
26 GOES-11 has five channels centered at 0.65, 3.9, 6.7, 10.7 and 12.0 μm . In the sampling region,
27 cloud property retrievals were produced at 15:15 and 15:45 UTC (Walther and Heidinger, 2012).

Deleted:

1 We chose the earlier time because it was more consistent with the MAS retrieval in terms of the
2 optical thickness along the ER-2 track. There are small discrepancies between the GOES and
3 MAS cloud top height retrievals, which are due to a combination of the different spatial
4 resolutions, and channels that are used for the respective retrievals (Walther and Heidinger, 2012;
5 Platnick et al., 2003; King et al., 2010). For the purpose of this study, these differences are not
6 significant.

7 Figure 2 shows the extended cloud scene (240 km × 240 km). Outside the MAS swath,
8 GOES-11 retrievals were used instead of those from MAS. Similarly, as for the sub-scene cloud,
9 the effective radius retrieval was extended throughout the vertical dimension. The optical
10 thickness was distributed vertically using the CRS profile with the closest match in column-
11 integrated water path (as compared to the retrieved value from GOES) and adjusted in altitude to
12 match the cloud top height retrievals from GOES-11. This approach for distributing profile
13 information from active instrumentation across the swath of a passive imager is more simplistic
14 than that developed by Barker et al. (2011) who used multi-spectral radiances from MODIS.
15 Transferring radar information to off-nadir pixels as far away as 120 km is not necessarily
16 justified due to spatial de-correlation of cloud systems (Miller et al., 2014). However, in the
17 absence of any other information, it was considered the best alternative to estimating the cloud
18 vertical structure without any *a priori* knowledge.

19 4. Model calculations

20 The calculations in this study were performed with the 3D Monte Carlo Atmospheric
21 Radiative Transfer Simulator (MCARaTS: Iwabuchi, 2006). MCARaTS is an open-source code
22 written in FORTRAN-90, which can be obtained at sites.google.com/site/mcarats/. It calculates
23 shortwave and longwave spectral or broadband radiances and irradiances based on a forward
24 propagating photon transport algorithm. It is optimized to run efficiently on parallel computers.

25 In addition to the two 3D cloud fields described in Section 3, the standard tropical
26 summer atmosphere as distributed within the libRadtran radiative transfer package
27 (www.libradtran.org; Mayer and Kylling, 2005) was used to prescribe the vertical profile of
28 temperature, pressure, water vapor, and other atmospheric gases. For gas molecular scattering, we

Deleted: , of which w

Deleted: one

1 calculated the optical thickness for each layer with the approximation by Bodhaine et al. (1999)
2 and used the built-in Rayleigh scattering phase function from MCARaTS. For gas molecular
3 absorption, we adopted the correlated k -distribution method described by Coddington et al.
4 (2008). It was originally based on Mlawer and Clough (1997), modified for the shortwave by
5 Bergstrom et al. (2003), and was specifically developed for the Solar Spectral Flux Radiometer
6 (SSFR: Pilewskie et al., 2003). The SSFR instrument line shape (6-8 nm full-width half-
7 maximum) defines the width of the channels in this study (narrower than MODIS or MAS
8 channels). The spectrum by Kurucz (1992) served as the extraterrestrial solar spectrum.

9 Calculations were performed at eleven wavelengths ranging from the near ultraviolet to
10 the very-near infrared (350, 400, 450, 500, 550, 600, 650, 700, 750, 800, 1000 nm) to capture the
11 spectral dependence of horizontal photon transport over a wide range of molecular scattering. At
12 1000 nm, molecular scattering is negligible and water vapor absorption is small; cloud absorption
13 is negligible for all wavelengths. For pixels dominated by ice clouds, the scattering phase
14 function and single scattering albedo were used from the general habit mixture of the ice cloud
15 bulk models developed by Baum et al. (2011) (parameterized by the effective radius). For liquid
16 water clouds (minority of cloud pixels), single scattering albedo and asymmetry parameter from
17 Mie calculations were used in conjunction with a Henyey-Greenstein phase function (which
18 generally simplifies irradiance calculations). In this study, all calculations were performed for an
19 ocean surface albedo (Coddington et al., 2010) and for a solar zenith angle of 35° for consistency
20 with the earlier publication by Schmidt et al. (2010). The solar azimuth angle was 60° (northeast).

21 The scene parameters (solar geometry, surface albedo, cloud properties) will be generalized in
22 future work (Song, 2016). For each wavelength, 10^{11} (10^{12}) photons were used for the sub-scene
23 (large-scale) cloud field, which corresponds to 7×10^6 (4×10^6) per pixel, respectively. MCARaTS
24 was run in the forward irradiance mode with periodic boundary conditions. For each 3D model
25 run, calculations were also performed using the independent pixel approximation (IPA) where
26 horizontal photon transport is deactivated.

Deleted: selected

Deleted: is

Formatted: Superscript

Formatted: Superscript

1 **5. Relationship between cloud spatial structure, net horizontal photon transport, and its**
2 **spectral dependence**

3 This section discusses the relationship between spatial structure and spectrally dependent
4 horizontal photon transport based on the small sub-scene. Since true absorption, A_λ , is negligible,
5 H_λ is equal to V_λ , the vertical flux divergence of an inhomogeneous cloud layer as defined in
6 Section 2, with $h_{\text{top}} \approx 13$ km and $h_{\text{base}} \approx 8$ km.

7 Table 1 shows the optical thickness and effective radius for the eight highlighted pixels
8 from Fig. 1 along with H_0 , the horizontal photon transport at $\lambda = 500$ nm, expressed in percent of
9 the incident irradiance. Positive values of H_0 are related to net photon loss to other pixels
10 (“radiation donors”), negative values to net photon gain (“radiation recipient” pixels). In the small
11 domain, values as high as 50% and as low as -125% were attained. When H_0 falls below -100%,
12 the radiation received through the sides of a column or voxel exceeds that from the top of the
13 domain. Table 1 is sorted by H_0 rather than by optical thickness. It shows immediately that there
14 is no relationship between the optical thickness (or cloud reflectance) and horizontal photon
15 transport. For example, pixel #6 is a “radiation donor,” whereas pixel #4 with roughly the same
16 optical thickness is a recipient. For the extreme case of zero cloud optical thickness, the effect of
17 horizontal photon transport had previously been observed as clear-sky radiance enhancement in
18 the vicinity of clouds (Wen et al., 2007; Kassianov and Ovtchinnikov, 2008; Várnai and Marshak,
19 2009; Marshak et al., 2014). Statistically, this enhancement is a function of the distance of a pixel
20 to the nearest cloud. However, the horizontal scale of this dependence varies with the spatial
21 context. Consequently, the distance to a certain cloud element cannot generally be used to
22 parameterize 3D cloud effects for individual pixels, whether cloud-free or cloud-covered. This is
23 illustrated when considering pixels #4-#8 in the anvil outflow, which have low optical thickness
24 (around 10) compared to the convective core (optical thickness ≥ 40) overflown from 15.45-15.48
25 UTC. The small contrasts in optical thickness (reflectance) between the pixels in close proximity
26 tend to drive the sign of H_0 to a greater extent than the exchange of radiation with the (bright)
27 core (for example, #6→#7, #5→#4, #7→#8, but not #5→#6). On the other hand, pixels #2 and
28 #3 have relatively low values of H_0 although they have the largest optical thickness of all eight

Deleted: H_0

Deleted: cannot exceed 100%, but may

Deleted: go

Deleted: in which case

Deleted: ,

Formatted: Not Highlight

Formatted: Not Highlight

1 pixels. While still donors, the magnitude of net horizontal flux to other pixels seems to be
2 diminished by the vicinity to the convective core. Overall, the direction, let alone the magnitude
3 of net horizontal flux, is difficult to predict from the distribution of optical thickness,
4 emphasizing 3D effects as a non-local phenomenon.

5 For the highlighted pixels in Table 1 (#5-#8), Fig. 3a shows the spectral shape of H_λ . The
6 absolute value H_λ increases with wavelength until it reaches an asymptotic value towards near-
7 infrared wavelengths, which we denote H_∞ . Donor pixels ($H_\lambda > 0$) are associated with a positive
8 spectral slope, $S_\lambda \equiv dH_\lambda/d\lambda > 0$; recipient pixels have a negative spectral slope. Remote sensing
9 studies (e.g., Marshak et al., 2008; Várnai and Marshak, 2009) had previously established that the
10 above-mentioned *radiance enhancement* for clear-sky pixels near clouds was associated with
11 “apparent bluing,” and proposed molecular scattering as the underlying cause for this spectral
12 dependence. To demonstrate that the same effect is at work here, molecular scattering was
13 deactivated in MCARaTS, keeping everything else the same in the calculations. In the resulting
14 spectra (* symbols in Fig. 3a), the wavelength dependence in the near-ultraviolet and visible
15 range disappears almost entirely, suggesting molecular scattering as the primary cause for the
16 spectral shape not only for clear-sky, but also for cloudy pixels. This begs the question (addressed
17 in the next section) of how it is possible to observe such a significant spectral effect for cloudy
18 pixels, given that cloud scattering outweighs molecular scattering by far. After turning molecular
19 scattering off, the remaining variability in H_λ is due to the weak dependence of cloud scattering
20 properties on wavelength and droplet or crystal effective radius, as well as minor gas absorption
21 features. Note that the earlier study by Schmidt et al. (2010) remained inconclusive as to the
22 mechanism of the spectral dependence they observed.

23 To first order, the spectral shape over the range of 350 to 650 nm can be characterized by
24 a single number—the spectral slope at $\lambda = 500$ nm, S_0 (obtained from a linear fit to $H_{\lambda=350-600}$
25 nm, included in Fig. 3a). Table 1 lists the value of S_0 for the eight pixels from Fig. 1, whereas Fig.
26 3b depicts the relationship between H_0 and S_0 for *every* pixel. It shows that not only the sign, but
27 also the magnitude of the net horizontal photon transport, is surprisingly well correlated with its
28 slope at 500 nm (in %/100 nm). This suggests that the phenomenon observed by Schmidt et al.

Deleted: s

Formatted: Font:Italic

Deleted: Δ

Deleted:

Deleted: ,

Deleted:)

1 (2010) for a few isolated data points is a general occurrence throughout a heterogeneous cloud
2 field. The close relationship between the magnitude and spectral shape of net horizontal photon
3 transport is the basis for the spectral parameterization of H_λ , developed in the next section.

4 In H_0 - S_0 space, all IPA calculations (red dots in Fig. 3b) are reduced to the origin because
5 they do not allow horizontal pixel-to-pixel radiation exchange by definition. Owing to periodic
6 boundary conditions, the domain average of H_0 is zero. The calculations without molecular
7 scattering (gray dots) confirm that molecular scattering dominates the spectral shape throughout
8 the domain. The vertical spread of the gray data points is due to the other factors mentioned
9 above (e.g., variability in cloud microphysics). To some extent, it is also apparent in the IPA
10 calculations.

Deleted: cloud

Deleted: H

Deleted: grey

Deleted: grey

11 6. Physical mechanism and parameterization

12 Our interpretation of Fig. 3 is that H_λ can be understood as the combination of two terms:

$$13 H_\lambda = H_\infty + \delta(\lambda). \quad (7)$$

Formatted: Font:Italic

14 1. The constant offset H_∞ is caused by column-to-column radiation exchange between cloud
15 elements. This is illustrated by Fig. 4, which shows the vertical profile of (a) downwelling,
16 (b) net, and (c) upwelling irradiance at 1000 nm wavelength for the cloud field from Fig. 1.
17 A change of net irradiance between altitudes z_0 and z_1 corresponds to net radiation loss or
18 gain within that layer. In this case, the domain-averaged profile of net irradiance (black line
19 in Fig. 4b) decreases slightly near the surface, due to small absorption in the wing of the 936
20 nm water vapor band. When subsampling over columns with a cloud optical thickness $\tau < 1$,
21 or $\tau > 120$, the 3D calculations differ from the IPA calculations because column-to-column
22 radiation transfer is enabled. Above the cloud field, columns with high cloud optical
23 thickness have higher reflectance than the domain average (Fig. 4c) and collectively lose
24 radiation to those with lower optical thickness; the opposite is true below the cloud where
25 columns with high optical thickness have lower transmittance (Fig. 4a). The magnitude of
26 the net horizontal photon transport (the difference of net irradiances at the bottom and top
27 altitude of a layer) increases with the geometrical layer thickness. Fig. 5 conceptually depicts

Deleted: that

Deleted: ⁶

Deleted:

Formatted: Font:Italic

Formatted: Font:Italic

1 the processes at work. Above clouds, net horizontal photon transport (reflected radiance,
2 projected into a horizontal plane) occurs from the high- to low-reflectance column. Below
3 clouds, the direction is reversed because the transmittance of thin clouds is larger than that of
4 thicker clouds. Note that below $\tau \approx 4$, directly transmitted radiation dominates the
5 downwelling irradiance, and the cloud may not act as a “diffuser” as shown in Fig. 5. The
6 direction of the green arrows is then along the direct beam. This simplified figure should *not*
7 be interpreted to suggest that the net horizontal transport generally occurs along gradients of
8 cloud optical thickness. As stated above, its direction and magnitude depends not only on
9 directly adjacent columns, but also on the large-scale context, which is why a
10 parameterization of 3D cloud effects in clear-sky areas in terms of the distance to the nearest
11 cloud is only possible in a statistical way, but not on an individual pixel basis (Wen et al.,
12 2007). The value of H_∞ can be obtained from H_λ for wavelengths where molecular scattering
13 becomes negligible and where cloud and gas absorption are small compared to H_λ : $A_\lambda \ll H_\lambda$.
14 For the purpose of this study, we chose $\lambda = 1000$ nm: $H_\infty \approx H_{\lambda=1000}$ nm.

- 15 2. The spectral perturbation δ_λ , superimposed on H_∞ , introduces the wavelength dependence of
16 H_λ . It is perhaps not immediately intuitive why molecular scattering would reduce the
17 magnitude of H_λ as indicated by the symbolic blue arrows in Fig. 5. Molecular scattering
18 essentially reduces the directionality of horizontal photon transport by redistributing
19 radiation, part of which can then be detected as enhanced clear-sky reflectance of clouds
20 (Marshak et al., 2008). A different, secondary process occurs when radiation is scattered out
21 of the direct beam in clear-sky areas into cloud shadows (dashed blue arrow in Fig. 5). It is
22 spectrally dependent as δ_λ but, unlike δ_λ , *independent* of H_∞ and its direction—thus
23 increasing the net radiation under both optically thick and thin clouds. For 550 nm
24 wavelength and shorter (not shown in Figure 4), the net irradiance does indeed increase
25 towards the surface, both for $\tau > 120$ and for $\tau < 1$. This secondary effect is not explicitly
26 captured by the first-order parameterization given below.

27 We express the proportionality of δ_λ to H_∞ as

Deleted: 7

Formatted: Font:Italic

Formatted: Font:Italic

$$\delta(\lambda) = -\varepsilon \left(\frac{\lambda}{\lambda_0} \right)^{-x} H_\infty \quad (\varepsilon \geq 0, \lambda_0 = 500 \text{ nm}), \quad (8)$$

where $(\lambda/\lambda_0)^{-x}$ describes the wavelength dependence, and ε is the constant of proportionality. The layer thickness for which H_λ is derived affects both H_∞ and δ_λ , but only marginally changes the correlation *between* them. Therefore, ε is a general parameter that can be used for relating spatial inhomogeneities and spectral signature of a cloud scene as a whole. It depends on scene parameters such as surface albedo, solar zenith angle, and cloud micro- and macrophysics (including vertical structure). This dependence is explored in a separate publication (Song, 2016). Using Eq. (8), the spectral slope S_0 can be derived as

$$S_0 = \left. \frac{dH_\lambda}{d\lambda} \right|_{\lambda=\lambda_0} = \left. \frac{d\delta(\lambda)}{d\lambda} \right|_{\lambda=\lambda_0} = x\varepsilon \frac{H_\infty}{\lambda_0}, \quad (9)$$

By combining Eqs. (7) and (8), one obtains $H_0 = H_{\lambda=500 \text{ nm}} = H_\infty(1 - \varepsilon)$, and Eq. (9) can be rewritten as

$$S_0 = \frac{x\varepsilon H_0}{1 - \varepsilon \lambda_0}, \quad (10)$$

where $x\varepsilon/(1 - \varepsilon)\lambda_0$ is the slope of the linear regression derived using all pixels in the cloud domain (for example, in Fig. 3b). Alternatively, one can derive both ε and x for each individual pixel from the regression of

$$\log \left(-\frac{\delta(\lambda)}{H_\infty} \right) = \log \varepsilon - x \log \frac{\lambda}{\lambda_0} \quad (11)$$

with $\log \varepsilon$ as intercept and x as slope, as shown in Fig. 6a. In this example, the fit parameter is about 4 as would be expected for molecular scattering as the underlying physical mechanism. The two-dimensional PDF $p(x, \varepsilon)$ for the population of pixels in the domain peaks at $\{x, \varepsilon\} \approx \{3.85, 0.065\}$ but has a considerable spread in both parameters, which is caused by pixels with negligible horizontal photon transport (and consequently large uncertainties in the fit parameters). The dashed lines in Fig. 3a show the fitted spectra (labeled “theoretical”) from this approach. For practical purposes, we fix $x \equiv 4$ for the remainder of this paper. This allows using

Formatted: Font:Italic

Deleted: and the secondary effect due to molecular scattering mentioned above will be

Deleted: follow-on

Deleted: from the previous section

Deleted: then

Formatted: Font:Italic

Deleted: the

Deleted: the

Deleted: i

Deleted: is

Formatted: Font:Italic

$$H_{\lambda} = H_{\infty} \left(1 - \varepsilon \left(\frac{\lambda}{\lambda_0} \right)^{-4} \right) \quad (12)$$

2 instead of Eq. (11) and deriving ε and H_{∞} for each pixel from a linear regression of H_{λ} versus
 3 $(\lambda/\lambda_0)^{-4}$ (i.e., H_{∞} is no longer a required input parameter as for the logarithmic regression). With
 4 ε known, S_0 can be calculated from Eq. (9). This is more accurate than the derivation of the slope
 5 from a linear fit to the spectrum as used for Fig. 3, which, due to the non-linearity of the spectral
 6 dependence, differs from that of the tangent if finite wavelength intervals are used. The domain-
 7 wide “effective” ε can then be derived from the slope of the regression line of S_0 versus H_0 for all
 8 pixels (Eq. (10) with $x = 4$). Fig. 7 shows the distribution of ε as derived from (12) for all those
 9 pixels with $\Delta(\varepsilon) < 5\%$. The median of this distribution (0.069) is almost identical to the
 10 “effective” value of ε (0.067). The standard deviation of the distribution is about 0.01. This
 11 means that the parameterized correlation between net horizontal transport and its spectral
 12 dependence can be applied to the domain as a whole as well as for individual pixels; if the
 13 spectral shape of H_{λ} is known, one can infer its magnitude throughout the near-ultraviolet and
 14 visible wavelength range. The correlation is robust regardless of the cloud context of a pixel,
 15 which is remarkable given the considerable variability in distance-based measures of 3D cloud
 16 effects (Várnai and Marshak, 2009).

17 Although our study was instigated by aircraft measurements, its findings are also relevant
 18 for satellite-based derivations of cloud radiative effects since the spectral perturbations δ_{λ}
 19 propagate into observed radiances (Song et al., 2016). This may be exploited in future
 20 applications for deriving correction terms for 3D radiative effects via their spectral signature.

21 The mean albedo of an inhomogeneous cloud field derived from CERES observations
 22 should be fairly insensitive to 3D effects because they are statistically folded into anisotropy
 23 models of such scene types (if these empirical models adequately accomplish the radiance-to-
 24 irradiance conversion for a range of sun-sensor geometries). By contrast, surface cloud radiative
 25 effects are much less constrained by direct CERES observations because cloud transmittance has
 26 to be derived from concomitant imagery. This is where biases introduced by H_{λ} are most
 27 significant. For the remainder of this paper, we therefore analyze the significance of H for

- Deleted: e
- Formatted: Font:Italic
- Formatted: Normal, Line spacing: exactly 22 pt
- Formatted: Font:Italic
- Formatted: Font:Italic
- Deleted: ⁸,
- Deleted: and a
- Deleted: H_{∞}
- Formatted: Font:Italic

- Deleted: -
- Formatted: Normal, Indent: First line: 0.5"
- Deleted: and imprint a spectral signature of H_{λ}
- Deleted: 5
- Deleted: In this context, it is important to emphasize the fundamental difference between radiance and irradiance and their observation from space and aircraft, respectively. Radiances are mainly affected by radiative smoothing and roughening within a cloud layer (e.g., Marshak et al., 2006). In addition, aircraft measurements also exhibit geometrical smoothing in their power spectra (Schmidt et al., 2007a), especially when acquired high above a cloud field. For this reason, radiance-derived cloud albedo products such as from aircraft imagers (Schmidt et al., 2007b; Kindel et al., 2010) often do not match their measured counterparts. Through our study, we now understand why this mismatch [Fig. 7 in Kindel et al., 2010] is associated with a spectral inconsistency in the albedo spectra (Schmidt and Pilewskie, 2012)—it can simply be explained by the term δ_{λ} in Eq. (7). ... [2]
- Deleted: empirical
- Deleted: ⁹

1 | varying degrees of spatial aggregation (Section 7), and make the connection to cloud
2 | transmittance (Section 8).

Deleted: ,

3 | 7. Scale dependence and spatial aggregation

4 | The results presented so far (e.g., in Fig. 3b) are based on calculations at a resolution of
5 | 0.5 km. The question is whether the correlation between the magnitude and spectral shape of H is
6 | scale invariant, and to what extent the effect of horizontal photon transport can be mitigated by
7 | spatial aggregation. To answer this question, we successively coarsened the pixel resolution to 15
8 | km, the largest super-pixel contained within the MAS swath (Fig. 1). Figure 8a shows that the
9 | correlation is indeed independent of the spatial aggregation scale and thus pixel size. The
10 | magnitude of H_0 decreases with pixel size: it ranges from +6% to -5% at 15 km resolution (close
11 | to CERES for nadir viewing), compared to about $\pm 50\%$ at 1-5 km (resolution of various MODIS
12 | level-2 products). Here, we use the large cloud scene (Fig. 2) to estimate for which aggregation
13 | scale beyond 15 km the magnitude of H_0 drops below the radiometric uncertainty of typical
14 | space- or ground-based radiometers (3-5%), at which point 3D cloud effects become insignificant
15 | from a practical point-of-view.

Deleted: Eq. (1) suggests that neglecting horizontal photon transport will cause biases in pixel-level products such as cloud transmittance and surface insolation. In the next section, we will examine to what extent horizontal photon transport translates into 3D-1D transmittance biases.

Deleted: radiative energy budget

16 | The results for the large scene, shown in Fig. 8b, confirm that the correlation is preserved
17 | for scales up to 70 km. However, H_0 at 15 km resolution varies from +17% to -13% throughout
18 | the large-scene domain, much more than in the MAS-only domain (+6% to -5%). One
19 | explanation for this larger range is the greater complexity of the large domain, providing a more
20 | extensive sample of cloud variability than the smaller sub-scene. This becomes quite clear when
21 | looking at the spatial distribution of horizontal photon transport: In Fig. 8c, we chose to plot S_0
22 | (y-axis in Fig. 8b) rather than H_0 . They are practically interchangeable thanks to the correlation
23 | between the two. The distribution of effective donor, recipient, and neutral regions (red, blue,
24 | green, respectively) bears almost no resemblance to the optical thickness field from Fig. 2. This
25 | demonstrates once again that horizontal photon transport cannot be derived from the spatial
26 | distribution of clouds in any simple way; strong contrasts between negative and positive H_0 (or
27 | S_0) can arise in optically thin boundary layer clouds (southwest corner of Fig. 2 and 8c) as well as
28 | in optically thick areas (deep convection, northeast corner of cloud scene). Considering the

Deleted:

Deleted: Extracting

1 GOES-MAS large-scene results within the boundaries of the MAS swath only (marked by the
2 green rectangle in Fig. 8c) allows estimating the net exchange of radiation between the MAS
3 domain and its large-scene context. The average value of H_0 within the small-scene subset is
4 +7.9%, which means that the small scene effectively loses photons to its surroundings. This
5 would not be detectable for such a large aggregation scale (where the entire MAS domain
6 represents a single “super-pixel”). This net energy export is not reproduced by the calculations
7 based on the MAS-only domain where the mean value of H_0 is zero, in keeping with energy
8 conservation that is satisfied by periodic boundary conditions in the radiative transfer model. The
9 range of H_0 in the MAS-only sub-scene of the GOES-MAS scene is +17% to -6% at 15 km
10 aggregation scale. This is still a larger range than obtained from the MAS-only calculations (+6%
11 to -5%), even after sub-setting the results from the large scene to the boundaries of the small
12 ones. The reason is simply that the 15 km super-pixel size is already half the width of the MAS-
13 only domain. Boundary conditions enforce the convergence of H_0 to zero as the area ratio of pixel
14 to domain size approaches 1, which causes an underestimation of the variability of H_0 for large
15 aggregation scales. By contrast, photons can also travel outside the confines of the domain in the
16 real world as represented by the larger GOES-MAS cloud scene in our study.

17 This is illustrated in Figure 8d, which shows the range of H_0 for both the large and the
18 small cloud scene as a function of aggregation scale. At small scales, the range is comparable for
19 the small and large scene. At 15 km aggregation scale, the range obtained from the small scene
20 has decreased to about half that of the large one. At 50 km pixel resolution, H_0 ranges from +7%
21 to -3% (+5% to -1% at 70 km). It is likely that the boundary conditions imposed on the large
22 domain also cause an underestimation of the H_0 variability at these large scales. Nevertheless,
23 these results suggest that above 60 km super-pixel size (about 3×3 CERES nadir footprints),
24 horizontal photon transport can be neglected for this cloud scene, based on a 3% uncertainty
25 threshold. This is only true when aggregating all native-resolution pixels, regardless of whether
26 they are flagged as clear sky or as cloud-covered. However, sampling cloudy and clear pixels
27 separately would result in much larger biases than 3% because high optical thickness pixels are
28 more likely to be effective photon donors than low-optical thickness or clear pixels, causing an

- Deleted: small
- Deleted: -only
- Deleted: scene
- Deleted: large-scale
- Deleted: of the small domain with its context

- Deleted: (
- Deleted:)

1 | asymmetry in the distribution of H_0 (Song et al., 2016).

2 | 8. Significance for Cloud Radiative Effect

3 | In this section, we evaluate the ramifications of net horizontal photon transport on
4 | estimates of cloud radiative effects. For any atmospheric column, H is connected to R and T
5 | through Eq. (1) and manifests itself in a transmittance and reflectance bias (λ index omitted):

$$6 | \Delta T = T^{IPA} - T^{3D} \quad (13a)$$

$$7 | \Delta R = R^{IPA} - R^{3D}. \quad (13a)$$

8 | Juxtaposing energy conservation for a horizontally homogeneous atmosphere ($T^{IPA} + R^{IPA} = 1$)
9 | with Eq. (1) for conservative scattering ($A=0$, therefore $T^{3D} + R^{3D} = 1 - H$) yields the plausible
10 | relationship

$$11 | H = \Delta T + \Delta R, \quad (14)$$

12 | which means that the error introduced by horizontal photon transport is partitioned into
13 | transmittance and reflectance bias. Since the bias ΔR is folded into the empirical radiance-to-
14 | irradiance conversion employed by CERES, we focus on ΔT in this study.

15 | For the eight super-pixels #11–#18 from Fig. 2, Fig. 9a shows the IPA bias ΔT , ranging
16 | from +2% to +14% in the mid-visible. Its spectral dependence is more complicated than the one
17 | shown for H in Fig. 3a, with a less obvious correlation between magnitude and spectral shape.
18 | Nevertheless, Fig. 9b shows a remarkable correlation between H_0 and ΔT_0 ($T^{IPA} - T^{3D}$ at 500
19 | nm) for the same aggregation scales as in Fig. 8b. For example, the H_0 range of +15% to –10%
20 | translates into +19% to –12% in ΔT_0 for a horizontal resolution of 20 km. Linear regression
21 | between H_0 and ΔT_0 suggests that in this case, H_0 propagates mainly into ΔT_0 , whereas it is
22 | uncorrelated with ΔR_0 for scales below 20 km (Fig. 10).

23 | For simplicity, the spectral dependence of ΔT as shown in Fig. 9a is approximated by

$$24 | \Delta T_\lambda = T_\lambda^{IPA} - T_\lambda^{3D} = \xi_0 \Big|_{350-600nm} \times (\lambda - \lambda_0) + (T_0^{IPA} - T_0^{3D}); \lambda_0 = 500 \text{ nm} \quad (15)$$

25 | where ξ_0 is the spectral slope of $T_\lambda^{IPA} - T_\lambda^{3D}$ calculated from the spectrum between 350 and 600
26 | nm. Fig. 9c shows that the spectral slopes of H and ΔT , S_0 and ξ_0 , are correlated despite the more

Formatted: Font:Italic

1 complicated spectral dependence of T compared to that of H (Fig. 9a). However, there is clearly
2 no 1:1 relationship as found between H_0 and ΔT_0 above. For example, $S_0 = -10\%/100$ nm
3 corresponds to only $\xi_0 = -6\%/100$ nm. This changes when extending the vertical layer boundaries
4 (8-13 km so far, bracketing only the cloud layer itself) to the atmosphere reaching from the
5 ground to cloud top. This distinction is indicated by carets above all quantities. This is slightly
6 different from the definition of \hat{T} in Section 2 where the upper boundary is the top of
7 atmosphere, not the top of the cloud. Fig. 9d not only shows a much stronger spectral dependence
8 of $\Delta\hat{T}$ (surpassing that of \hat{H}) compared to that of ΔT and H in Fig. 9c, but also that the
9 correlation is no longer scale invariant. This means that the vertical bracket for deriving T , R , and
10 H has to be chosen with consideration of the vertical location of the cloud layer. By contrast, the
11 correlation between H and S as discussed in Section 6 is fairly independent of the layer
12 boundaries.

Deleted: hat

13 For future studies of IPA-3D biases in satellite-derived estimates of surface cloud
14 radiative effects, Fig. 4b suggests the center of a cloud as upper boundary of the bracket where
15 $|dF_{net}/dz|$ reaches a domain-wide minimum because 3D effects can be vertically separated into a
16 transmittance and reflectance part below and above this level, respectively. Moreover, the
17 correlation between ΔT and its spectral dependence ξ_0 (not shown) can be exploited to detect
18 IPA-3D biases in ground-based irradiance measurements below cloud fields (Song, 2016). While
19 our study suggests that horizontal photon transport mainly propagates into transmittance biases,
20 there is some indication (Fig. 10) that at scales above 20 km, non-zero values of H_0 translate into
21 albedo (reflected irradiance) biases as well. This increasing correlation with scale is probably
22 associated with the gradual de-correlation between \hat{S}_0 and $\hat{\xi}_0$ observed in Fig. 9b. In order to
23 improve satellite-based estimates of cloud radiative effects, it is important to understand how H_0
24 is partitioned into ΔT and ΔR [Eq. (14)] at different aggregation scales. A detailed study would
25 need to be conducted for different cloud morphologies, sun angles, and surface albedos and is left
26 for the future.

Deleted: where

Deleted: Meanwhile, Song et al. (2015) investigate the link between net horizontal transport in cloud fields and spectral perturbations in reflected *radiance*.

27 9. Summary and conclusions

28 Deriving the radiative effects of inhomogeneous cloud scenes from observations by

1 satellite, aircraft, or at the surface is often portrayed as an intractable problem because it cannot
2 be accomplished by isolating a pixel from its spatial context. At the core of the issue is pixel-to-
3 pixel exchange of radiation, or net horizontal photon transport, which occurs over a range of
4 scales. The original motivation for this study was to gain a physical understanding of this
5 phenomenon's spectral dependence in the near-ultraviolet and visible wavelength range, which
6 had been found in aircraft irradiance observations (Schmidt et al., 2010). We were able to identify
7 molecular scattering as the underlying mechanism for the spectral dependence using three-
8 dimensional radiative transfer calculations with cloud imagery and radar observations as input.
9 When de-activating molecular scattering in the radiative transfer model, the wavelength
10 dependence disappeared almost entirely in the vertical flux divergence V , which comprises net
11 horizontal flux density H as well as true layer absorption A . To simplify the analysis, we limited
12 our study to conservative scattering by choosing wavelengths with negligible gas or cloud
13 absorption ($A \approx 0$), and by excluding aerosols. When activated in the model, molecular scattering
14 manifested itself as a spectral perturbation (more accurately: modulation) δ_λ to an otherwise
15 *spectrally neutral* horizontal flux density H_∞ , which in turn could be traced back to horizontal
16 exchange of radiation due to spatial inhomogeneity of cloud elements within the domain. Beyond
17 the original scope of this study, we made a few surprising discoveries:

- 18 1. The spectral perturbation δ_λ is not independent of the spectrally neutral part H_∞ caused by
19 the clouds themselves. Instead, the mid-visible spectral slope of H_λ is correlated with H itself
20 (i.e., with the magnitude of the spectrally neutral part H_∞), which led to the simple
21 parameterization

$$22 \quad \delta_\lambda = -\varepsilon \left(\frac{\lambda}{\lambda_0} \right)^{-x} H_\infty .$$

- 23 2. We were able to show that the exponent x is close to 4, which further confirmed molecular
24 scattering as the dominating physical mechanism behind the spectral perturbation. The
25 constant of proportionality, ε , can be regarded as universally valid for all pixels within the
26 cloud domain, independently of the vertical or horizontal spatial distribution of clouds. This
27 means that the spectrally dependent horizontal photon transport can be represented as

$$H_\lambda = H_\infty + \delta_\lambda = H_\infty \left(1 - \varepsilon \left(\frac{\lambda}{\lambda_0} \right)^{-4} \right)$$

for *each pixel* within the domain with $\varepsilon = 0.7 \pm 0.1$ for the scene we studied. It seems remarkable that one single value of ε should suffice to describe the relationship between the magnitude of H (caused by clouds) and its spectral dependence (imprinted on H by a completely different physical process, molecular scattering) – especially considering the range of different clouds within the domain. The correlation holds for each pixel, no matter what its spatial context may be. Once ε is established for a given cloud scene, the spectral perturbations associated with horizontal photon transport can be derived for each pixel if the value of H_0 is known. Conversely, if the spectral shape of H_λ is known at one wavelength, its magnitude can easily be inferred for the whole spectrum. This may be especially significant considering that H cannot be directly observed from space. It is likely that the spectral perturbations will propagate into the observed radiances. Indeed, Song et al. (2016) found evidence of this connection in aircraft data, which had previously been reported by Várnai and Marshak (2009) in clear-sky satellite observations near clouds. The close correlation that we found in our study may be a future pathway to inferring the magnitude of H from its spectral manifestation in the observed radiances.

3. The correlation and parameterization hold for a range of spatial aggregation scales, and are fairly independent of the location of the bracketing altitudes that define the layer. This scale invariance only breaks down when extending a layer very close to the surface where a secondary spectral effect has to be factored in (see Section 6 and dashed arrow in Figure 5).
4. The observed correlation between H and its spectral shape can also be found between transmitted irradiance T and its spectral shape, although it is not scale invariant beyond 20 km.
5. H is correlated with ΔT , the IPA transmittance bias for each pixel, but not with ΔR (at least at small scales). This means that 3D cloud effects in the form of horizontal photon transport translate almost exclusively into a transmittance bias. At scales above 20 km, a correlation between H and ΔR does emerge, which requires further study. The correlation between H

- Deleted: H
- Deleted: H
- Deleted: the
- Deleted: value
- Deleted: of H
- Deleted: 5
- Deleted: .
- Deleted: In fact,
- Deleted: previously reported this effect
- Deleted: radiance

1 and ΔT can potentially be exploited for ground-based spectral irradiance observations (Song,
2 2016).

3 Few of these findings could be expected at the outset of our research, and they evoke a number of
4 new questions:

5 1. How does the discovered correlation and the constant of proportionality in its
6 parameterization, ε , depend on scene parameters such as solar zenith and azimuth angle,
7 surface albedo (magnitude and spectral dependence), and cloud morphology and
8 microphysics? What “drives” the parameter ε ?

9 2. Can the spectral perturbations associated with H indeed be detected in reflected radiances,
10 and can they be used to infer the magnitude of H indirectly?

11 3. Can the findings for the near-ultraviolet and visible wavelength range be generalized to the
12 near-infrared wavelength range where clouds and atmospheric gases do absorb?

13 4. What are the implications of our findings for estimating aerosol radiative effects (such as
14 heating rates) in presence of inhomogeneous cloud fields?

15 5. Can the method by Ackerman and Cox (1981) to correct for horizontal photon transport in
16 aircraft measurements of atmospheric absorption by using a visible channel as basis for the
17 correction of near-infrared absorption be upheld for future measurements, even in the
18 modified form proposed by Kassianov and Kogan (2002)?

19 6. Can H and ΔT be derived from spectral perturbations in transmitted irradiance observations
20 by ground-based spectrometers?

21 Question 2 will be partially addressed by Song et al. (2016); questions 1, 3, 5, and 6 are discussed
22 by Song (2016) and will be further investigated in future publications. Furthermore, questions 3
23 and 4 are the subjects of active research in the framework of an ongoing or planned field missions
24 (NASA ORACLES and CAMP2Ex). This publication constitutes a further contribution to the
25 emerging field of cloud-aerosol spectroscopy (Schmidt and Pilewskie, 2012), which is expected
26 to improve the estimation of cloud-aerosol parameters and their radiative effects through
27 spectrally resolved observations from the ground, aircraft, and, ultimately, space.

28

Deleted:

Deleted: its

Deleted: 5

Deleted: NSF ONFIRE

Deleted: , dedicated to the radiative effects and remote sensing of aerosol in vicinity to clouds

1 **Acknowledgements**

2 The research presented in this paper was supported by grants NNX14AP72G (Shi Song and
3 Sebastian Schmidt) and NNX12AC41G (Michael King) within the NASA radiation sciences
4 program. The calculations were performed on the supercomputer “Janus”, which is supported by
5 the US National Science Foundation (award number CNS-0821794) and the University of
6 Colorado Boulder. It is a joint effort of the University of Colorado Boulder, the University of
7 Colorado Denver, and the National Center for Atmospheric Research. Janus is operated by the
8 University of Colorado Boulder. We appreciate the effort of Thomas Arnold (NASA Goddard
9 Space Flight Center) in supporting the MAS calibrations and retrievals.

Deleted: NASA
Deleted: “Linking the Radiative Energy Budget and Remote Sensing of Cloud and Aerosol Fields”

Deleted: -

1 **References**

- 2 Ackerman, S. A., and Cox, S. K.: Aircraft observations of shortwave fractional absorptance of
3 non-homogeneous clouds, *J. Appl. Meteorol.*, 20, 1510-1515, 1981.
- 4 Arking, A.: The influence of clouds and water vapor on atmospheric absorption, *Geophys. Res.*
5 *Lett.*, 26, 2729-2732, 1981.
- 6 Barker, H. W., Jerg, M. P., Wehr, T., Kato, S.: Donovan D. P., and Hogan R. J.: A 3D cloud-
7 construction algorithm for the EarthCARE satellite mission. *Q. J. Roy. Meteorol. Soc.*, 137,
8 1042-1058, 2011.
- 9 Barker, H. W., Kato, S., and Wehr, T.: Computation of solar radiative fluxes by 1D and 3D
10 methods using cloudy atmospheres inferred from A-train satellite data, *Surv. Geophys.*, 33,
11 657-676, 2012.
- 12 Baum, B. A., Yang, P., Heymsfield, A. J., Schmitt, C., Xie, Y., Bansemer, A., Hu, Y. X., and
13 Zhang, Z.: Improvements to shortwave bulk scattering and absorption models for the remote
14 sensing of ice clouds. *J. Appl. Meteor. Climatol.*, 50, 1037-1056, 2011.
- 15 Bergstrom, R. W., Pilewskie, P., Schmid, B., and Russell, P. B.: Estimates of the spectral aerosol
16 single scattering albedo and aerosol radiative effects during SAFARI 2000, *J. Geophys. Res.*,
17 108, 8474, doi:10.1029/2002JD002435, 2003.
- 18 Bodhaine, B. A., Wood, N. B., Dutton, E. G., and Slusser, J. R.: On Rayleigh optical depth
19 calculations, *J. Atmos. and Ocean. Tech.*, 16, 1854-1861, 1999.
- 20 Coddington, O., Schmidt, K. S., Pilewskie, P., Gore, W. J., Bergstrom, R. W., Roman, M.,
21 Redemann, J., Russell, P. B., Liu, J., and Schaaf, C. C.: Aircraft measurements of spectral
22 surface albedo and its consistency with ground-based and space-borne observations, *J.*
23 *Geophys. Res.*, 113, D17209, doi:10.1029/2008JD010089, 2008.
- 24 Coddington, O. M., Pilewskie, P., Redemann, J., Platnick, S., Russell, P. B., Schmidt, K. S.,
25 Gore, W. J., Livingston, J., Wind, G., and Vukicevic, T.: Examining the impact of overlying
26 aerosols on the retrieval of cloud optical properties from passive remote sensing, *J. Geophys.*
27 *Res.*, 115, D10211, doi:10.1029/2009JD012829, 2010.
- 28 Fritz, S., and MacDonald, T. H.: Measurements of absorption of solar radiation by clouds, *Bull.*

1 Am. Meteorol. Soc., 32, 205-209, 1951.

2 Ham, S.-H., Kato, S., Barker, H. W., Rose, F. G., and Sun-Mack, S.: Effects of 3-D clouds on
3 atmospheric transmission of solar radiation: Cloud type dependencies inferred from A-train
4 satellite data, *J. Geophys. Res.*, 119, 943-963, 2014.

5 Illingworth, A. J., Barker, H. W., Beljaars, A., Ceccaldi, M., Chepfer, H., Clerbaux, N., Cole, J.,
6 Delanoë, J., Domenech, C., Donovan, D. P., Fukuda, S., Hiraoka, M., Hogan, R. J.,
7 Huenerbein, A., Kollias, P., Kubota, T., Nakajima, T., Nakajima, T. Y., Nishizawa, T.,
8 Ohno, Y., Okamoto, H., Oki, R., Sato, K., Satoh, M., Shephard, M. W., Velázquez-Blázquez,
9 A., Wandinger, U., Wehr, T., and van Zadelhoff, G.-J.: The EarthCARE Satellite: The Next
10 Step Forward in Global Measurements of Clouds, Aerosols, Precipitation, and Radiation.
11 *Bull. Amer. Meteor. Soc.*, 96, 1311–1332, doi: [http://dx.doi.org/10.1175/BAMS-D-12-](http://dx.doi.org/10.1175/BAMS-D-12-00227.1)
12 [00227.1](http://dx.doi.org/10.1175/BAMS-D-12-00227.1), 2015.

13 Iwabuchi, H.: Efficient Monte Carlo methods for radiative transfer modeling. *J Atmos. Sci.*, 63,
14 2324-2339, 2006.

15 Kassianov, E. I., and Kogan, Y. L.: Spectral dependence of radiative horizontal transport in
16 stratocumulus clouds and its effect on near-IR absorption, *J. Geophys. Res.*, 107(D23), 4712,
17 doi:10.1029/2002JD002103, 2002.

18 [Kassianov E. I., and Ovtchinnikov, M.: On reflectance ratios and aerosol optical depth retrieval in
19 the presence of cumulus clouds. *Geophys. Res. Lett.*, 35:L06807.
20 <http://dx.doi.org/10.1029/2008GL033231>, 2008.](http://dx.doi.org/10.1029/2008GL033231)

21 Kato, S., Loeb, N. G., Rose, F. G., Doelling, D. R., Rutan, D. A., Caldwell, T. E., Yu, L., and
22 Weller, R. A.: Surface irradiances consistent with CERES-derived top-of-atmosphere
23 shortwave and longwave irradiances, *J. Clim.*, 26, 2719-2740, 2013.

24 Kindel, B. C., Schmidt, K. S., Pilewskie, P., Baum, B. A., Yang, P., and Platnick, S.:
25 Observations and modeling of ice cloud shortwave spectral albedo during the Tropical
26 Composition, Cloud and Climate Coupling Experiment (TC⁴), *J. Geophys. Res.*, 115,
27 D00J18, doi:10.1029/2009JD013127, 2010.

28 Kindel, B. C., Pilewskie, P., Schmidt, K. S., Coddington, O. M., and King, M. D.: Solar spectral

1 absorption by marine stratus clouds: Measurements and modeling, *J. Geophys. Res.*, 116,
2 D10203, doi:10.1029/2010JD015071, 2011.

3 King, M. D., Menzel, W. P., Grant, P. S., Myers, J. S., Arnold, G. T., Platnick, S. E., Gumley, L.
4 E., Tsay, S. C., Moeller, C. C., Fitzgerald, M., Brown, K. S., and Osterwisch, F. G.: Airborne
5 scanning spectrometer for remote sensing of cloud, aerosol, water vapor and surface
6 properties, *J. Atmos. Ocean. Tech.*, 13, 777-794, 1996.

7 King, M. D., Platnick, S., Wind, G., Arnold, G. T., and Dominguez, R. T.: Remote sensing of
8 radiative and microphysical properties of clouds during TC⁴: Results from MAS, MASTER,
9 MODIS, and MISR, *J. Geophys. Res.*, 115, D00J07, doi:10.1029/2009JD013277, 2010.

10 Kurucz, R. L.: Synthetic infrared spectra, in *Infrared Solar Physics: Proceedings of the 154th*
11 *Symposium of the International Astronomical Union*, edited by D. M. Rabin, J. T. Jefferies,
12 and C. Lindsey, pp. 523-531, Kluwer Acad., Dordrecht, Netherlands, 1992.

13 Li, L., Heymsfield, G. M., Racette, P. E., Tian, L., and Zenker, E.: A 94 GHz cloud radar system
14 on a NASA high-altitude ER-2 aircraft, *J. Atmos. Oceanic Technol.*, 21, 1378-1388, 2004.

15 Liu, C., and Illingworth, A.: Toward more accurate retrievals of ice water content from radar
16 measurements of clouds, *J. Appl. Meteorol.*, 39, 1130-1146, 2000.

17 Loeb N. G., Kato, S., Loukachine, K., and Smith, N. M.: Angular distribution models for top-of-
18 atmosphere radiative flux estimation from the clouds and the earth's radiant energy system
19 instrument on the Terra satellite. Part I: Methodology, *J Atmos. Oceanic Technol.* 22, 338-
20 351, 2005.

21 Marshak, A., and Davis, A.: *3-D Radiative Transfer in Cloudy Atmospheres*, Springer, ISBN-13
22 978-3-540-23958-1, 2005.

23 Marshak, A., Platnick, S., Várnai, T., Wen, G., and Cahalan, R. F.: Impact of three-dimensional
24 radiative effects on satellite retrievals of cloud droplet sizes, *J. Geophys. Res.*, 111, D09207,
25 doi:10.1029/ 996 2005JD006686, 2006.

26 Marshak, A., Wen, G., Coakley, J. A., Jr., Remer, L. A., Loeb, N. G., and Cahalan, R. F.: A
27 simple model for the cloud adjacency effect and the apparent bluing of aerosols near clouds,
28 *J. Geophys. Res.*, 113, D14S17, doi:10.1029/2007JD009196, 2008.

Deleted: -

... [3]

1 Marshak, A., Wiscombe, W., Davis, A., Oreopoulos, L., and Cahalan, R.: On the removal of the
2 effect of horizontal fluxes in two-aircraft measurements of cloud absorption, *Quart. J. Roy.*
3 *Meteorol. Soc.*, 125, 2153–2170, 1999.

4 [Marshak, A., Evans, F. E., Várnai, T., Wen, G.: Extending 3D near-cloud corrections from](#)
5 [shorter to longer wavelengths, *J. Quant. Spectroscopy* 147, 79-85, 2014.](#)

6 Mayer, B., and Kylling, A.: Technical note: The libRadtran software package for radiative
7 transfer calculations—Description and examples of use, *Atmos. Chem. Phys.*, 5, 1855-1877,
8 2005.

9 Miller, S. D., Forsythe, J. M., Partain, P. T., Haynes, J. M., Bankert, R. L., Sengupta, M.,
10 Mitrescu, C., Hawkins, J. D., and Vonder Haar, T. H.: Estimating three-dimensional cloud
11 structure via statistically blended satellite observations. *J. Appl. Meteor. Climatol.*, 53, 437-
12 455, 2014.

13 Minnis, P., Sun-Mack, S., Young, D. F., Heck, P. W., Garber, D. P., Chen, Y., Spangenberg, D.
14 A., Arduini, R. F., Trepte, Q. Z., Smith, W. L. Jr., Ayers, J. K., Gibson, S. C., Miller, W. F.,
15 Hong, G., Chakrapani, V., Takano, Y., Liou, K. N., Xie, Y., and Yang, P.: CERES edition-2
16 cloud property retrievals using TRMM VIRS and Terra and Aqua MODIS data—Part I:
17 Algorithms, *IEEE Trans. Geosci. Remote Sens.*, 49(11), 4374–4400, 2011.

18 Mlawer, E., and Clough, S. A.: On the extension of rapid radiative transfer model to the
19 shortwave region, in *Proc. Sixth ARM Science Team Meeting*, pp. 223–226, Atmospheric
20 Radiation Measurement (ARM) Program, San Antonio, TX, conf-9603149, 1997.

21 Pilewskie, P., Pommier, J., Bergstrom, R., Gore, W., Rabbette, M., Howard, S., Schmid, B., and
22 Hobbs, P. V.: Solar spectral radiative forcing during the South African Regional Science
23 Initiative, *J. Geophys. Res.*, 108, 8486, doi:10.1029/2002JD002411, 2003.

24 Platnick, S.: Approximations for horizontal photon transport in cloud remote sensing problems, *J.*
25 *Quant. Spectrosc. Radiat. Transfer*, 68(1), 75-99, 2001.

26 [Platnick, S., M. D. King, S. A. Ackerman, W. P. Menzel, B. A. Baum, J. C. Riedi, and R. A.](#)
27 [Frey, 2003: The MODIS cloud products: Algorithms and examples from Terra. *IEEE Trans.*](#)
28 [Geosci. Remote Sens.](#), 41, 459–473.

1 | Scheirer, R., and Macke, A.: Cloud inhomogeneity and broadband solar fluxes, *J. Geophys. Res.*,
2 | 108, 4599, doi:10.1029/2002JD003321, D19, 2003.

3 | Schmidt, K. S., Venema, V., Di Giuseppe, F., Scheirer, R., Wendisch, M., and Pilewskie, P.:
4 | Reproducing cloud microphysical and irradiance measurements using three 3D cloud
5 | generators, *Quart. J. Roy. Meteorol. Soc.*, 133, 765-780, 2007a.

6 | Schmidt, K. S., Pilewskie, P., Platnick, S., Wind, G., Yang, P., and Wendisch, M.: Comparing
7 | irradiance fields derived from Moderate Resolution Imaging Spectroradiometer airborne
8 | simulator cirrus cloud retrievals with solar spectral flux radiometer measurements, *J.*
9 | *Geophys. Res.*, 112, D24206, doi:10.1029/2007JD008711, 2007b.

10 | Schmidt, K. S., Pilewskie, P., Mayer, B., Wendisch, M., Kindel, B., Platnick, S., King, M. D.,
11 | Wind, G., Arnold, G. T., Tian, L., Heymsfield, G., and Kalesse, H.: Apparent absorption of
12 | solar spectral irradiance in heterogeneous ice clouds, *J. Geophys. Res.*, 115, D00J22,
13 | doi:10.1029/2009JD013124, 2010.

14 | Schmidt, K. S., and Pilewskie, P.: Airborne Measurements of Spectral Shortwave Radiation in
15 | Cloud and Aerosol Remote Sensing and Energy Budget Studies, in *Light Scattering*
16 | *Reviews*, 6, A. Kokhanovsky (ed.), Springer, 2012.

17 | Schmidt, K. S., Song, S., Feingold, G., Pilewskie, P., Coddington, O., 2014: Relating shortwave
18 | passive remote sensing and radiative effects in aerosol-immersed broken cloud fields, *AMS*
19 | *conference, Boston, July 2014*.
20 | <https://ams.confex.com/ams/14CLOUD14ATRAD/webprogram/Paper250570.html>

21 | Stephens, G. L., Tsay, S.-C., Stackhouse Jr., P. W., and Flatau, P. J.: The relevance of the
22 | microphysical and radiative properties of cirrus clouds to climate and climatic feedback, *J.*
23 | *Atmos. Sci.*, 47, 1742-1753, 1990.

24 | Song, S., Schmidt, K. S., Pilewskie, P., King, M. D., and Platnick, S.: Quantifying the spectral
25 | signature of heterogeneous clouds in shortwave radiation measurements during the Studies
26 | of Emissions and Atmospheric Composition, Clouds and Climate Coupling by Regional
27 | Surveys (SEAC⁴RS), to be submitted to *J. Geophys. Res.*, 2016.

28 | Song, S.: The spectral signature of cloud spatial structure in shortwave radiation. *Ph.D. thesis*,

Deleted: -

Formatted: Superscript

Deleted: 5

Formatted: Font:Italic

1 [Department of Atmospheric and Oceanic Sciences, University of Colorado Boulder, USA,](#)
2 [138 pp., 2016,](#)

Deleted: University of Colorado Boulder,
USA, 2016

- 3 Titov, G. A.: Radiative horizontal transport and absorption in stratocumulus clouds, *J. Atmos.*
4 *Res.*, 55, 2549-2560, 1998.
- 5 Toon O. B., Starr, D. O., Jensen, E. J., Newman, P. A., Platnick, S., Schoeberl, M. R., Wennberg,
6 P. O., Wofsy, S. C., Kurylo, M. J., Maring, H., Jucks, K. W., Craig, M. S., Vasques, M. F.,
7 Pfister, L., Rosenlof, K. H., Selkirk, H. B., Colarco, P. R., Kawa, S. R., Mace, G. G., Minnis,
8 P., and Pickering, K. E.: Planning, implementation, and first results of the Tropical
9 Composition, Cloud and Climate Coupling Experiment (TC⁴), *J. Geophys. Res.*, 115,
10 D00J04, doi:10.1029/2009JD013073, 2010.
- 11 Várnai, T., and Marshak, A.: MODIS observations of enhanced clear sky reflectance near clouds,
12 *Geophys. Res. Lett.*, 36, L06807, doi:10.1029/2008GL037089, 2009.
- 13 Walther, A., and Heidinger, A.: Implementation of the Daytime Cloud Optical and Microphysical
14 Properties Algorithm (DCOMP) in PATMOS-x. *J. Appl. Meteor. Climatol.*, 51, 1371-1390,
15 2012.
- 16 Welch, R. M., Cox, S. K. and Davis, J. M.: Solar Radiation and Clouds. *Meteor. Monogr.*, No.
17 39, Amer. Meteor. Soc., 93 pp., 1980.
- 18 Wen, G., Marshak, A., Cahalan, R. F., Remer, L. A., and Kleidman, R. G.: 3-D aerosol-cloud
19 radiative interaction observed in collocated MODIS and ASTER images of cumulus cloud
20 fields, *J. Geophys. Res.*, 112, D13204, doi:10.1029/2006JD008267, 2007.
- 21 Wielicki, B. A., Barkstrom, B. R., Harrison, E. F., Lee, R. B., Smith, G. L., and Cooper, J. E.:
22 Clouds and the Earth's Radiant Energy System (CERES): An Earth Observing System
23 Experiment, *Bull. Amer. Meteor. Soc.*, 77, 853-868, 1996.
- 24 Wiscombe, W. J., Welch, R. M., and Hall, W. D.: The effects of very large drops on cloud
25 absorption, part I: Parcel models, *J. Atmos. Sci.*, 41, 1336-1355, 1984.
- 26
27

1 | **Table 1.** Cloud optical thickness τ , effective radius r_e , and values of H_0 and S_0 for the eight
 2 pixels highlighted in Fig. 1 (sorted by H_0). For pixels 5, 6, 7, 8, Fig. 3a shows the spectral shape
 3 of H_λ .

Pixel	τ	r_e (μm)	H_0 (%)	S_0 (%/100 nm)
6	10.3	27.5	28.92	2.36
1	13.0	30.1	21.17	1.56
3	21.2	30.0	13.04	1.08
2	18.1	30.6	9.92	1.63
5	12.2	27.5	4.95	0.48
7	8.0	27.8	-5.18	-0.78
4	11.8	28.2	-18.7	-1.54
8	7.7	24.2	-24.13	-2.46

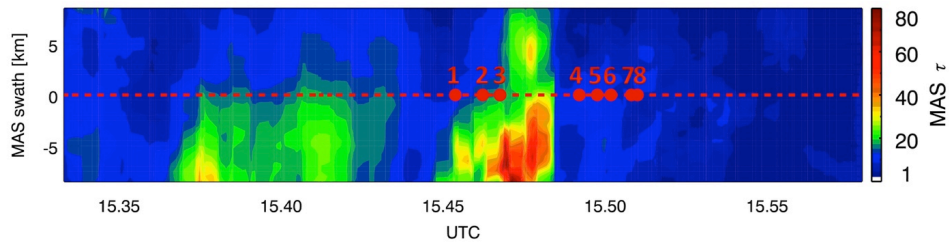
Deleted: H_0

Deleted: S_0

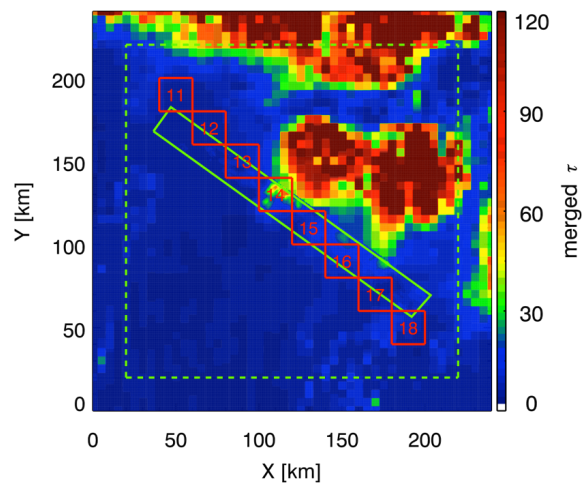
Formatted: Font:Italic

Formatted: Font:(Default) Times New Roman, Not Bold, Italic, Font color: Auto

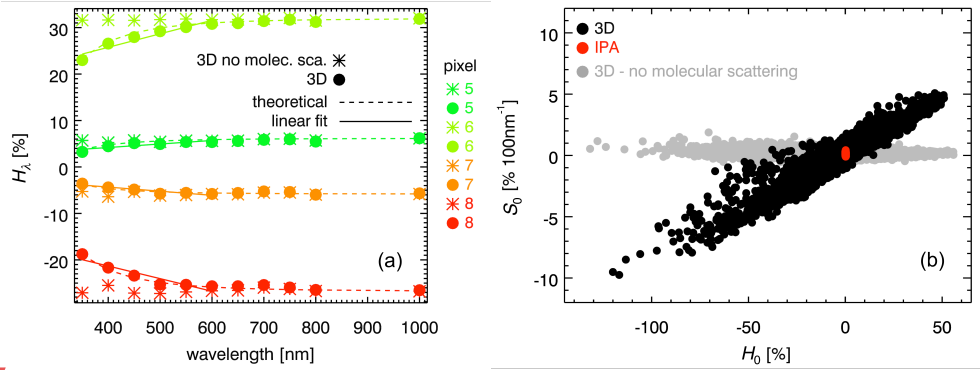
4



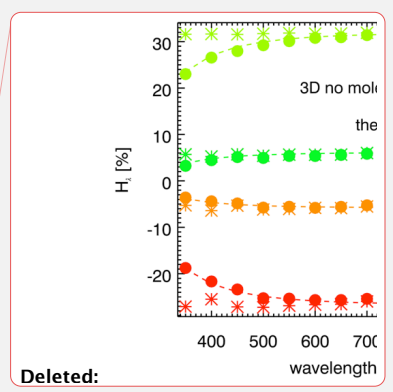
1
 2 **Fig. 1.** Cloud optical thickness from MAS along an ER-2 leg from 17 July 2007 (length: 192 km,
 3 swath: 17.5 km), re-gridded to a horizontal resolution of 500 m. The red dashed line indicates the
 4 ER-2 flight track in the center of the MAS swath. Results of net horizontal photon transport for
 5 the eight highlighted pixels are shown in Table 1 and Fig. 3a.



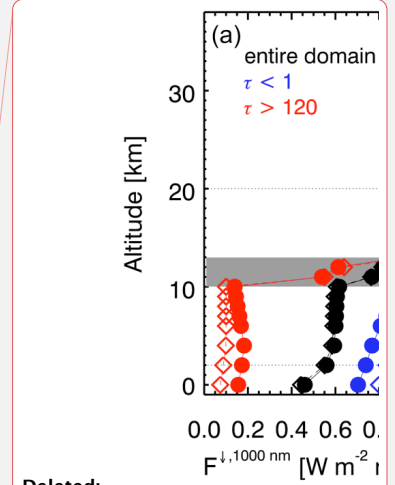
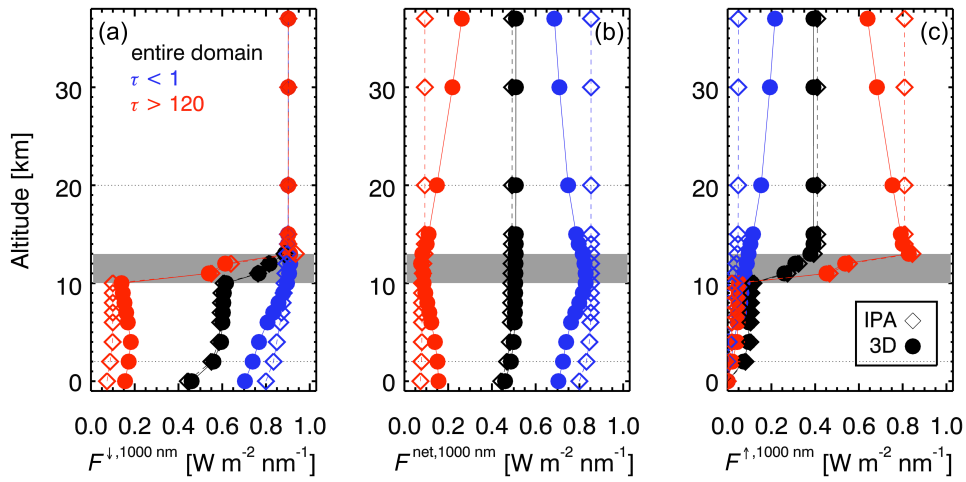
1
 2 **Fig. 2.** Optical thickness of the large-scale cloud field. The green rectangle marks the embedded
 3 MAS swath (Fig. 1); the red squares mark 20 km “super-pixels” within the scene. Radiative
 4 transfer model output outside the dashed green square is discarded (see Section 7).



1
 2 **Fig. 3.** (a) The H_λ spectra of pixels {5,6,7,8} from Fig. 1 and Table 1 with (•) and without (*)
 3 molecular scattering in the 3D calculations, as well as a fit based on Eq. (12) from Section 6
 4 (dashed lines) and the simplified linear fit for obtaining S_0 (solid lines). (b) Spectral slope (S_0) vs.
 5 net horizontal photon transport (H_0) from (a) (both at 500 nm) for all the pixels from Fig. 1. Only
 6 3D calculations with molecular scattering (black dots) show the systematic correlation between
 7 H_0 and S_0 . Disabling molecular scattering (gray dots) incorrectly predicts a spectrally neutral
 8 (flat) H_λ ($S_0 \approx 0$ for all pixels). By definition, 1D calculations (IPA, red dots) do not reproduce
 9 net horizontal photon transport at all ($H_0 = 0$ for all pixels).



Deleted: grey



Deleted:

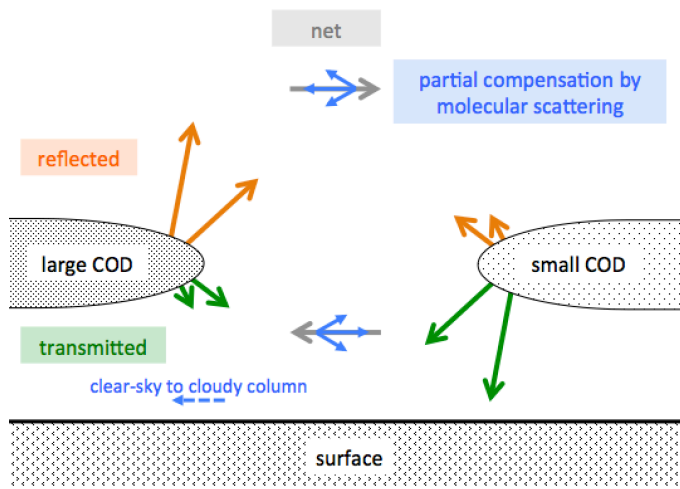
Deleted: grey

Deleted: τ

Deleted: .

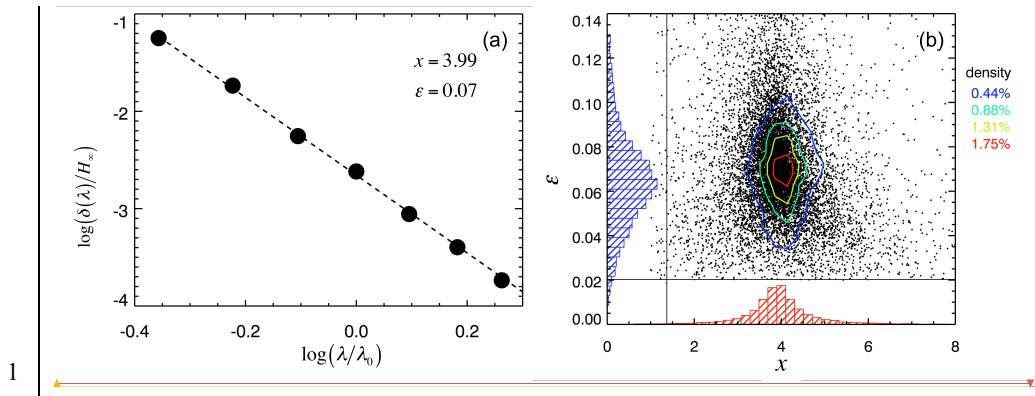
Formatted: Font:Italic

1
2 **Fig. 4.** Profiles of (a) downwelling, (b) net, and (c) upwelling irradiance at 1000 nm for the cloud
3 field from Fig. 1. The location of the cloud layer is marked in gray. Both IPA (dashed line,
4 hollow symbols) and 3D calculations (solid line, full symbols) are shown, averaged over the full
5 domain (black), over all columns with $\tau < 1$ (blue) and over columns with $\tau > 120$ (red).

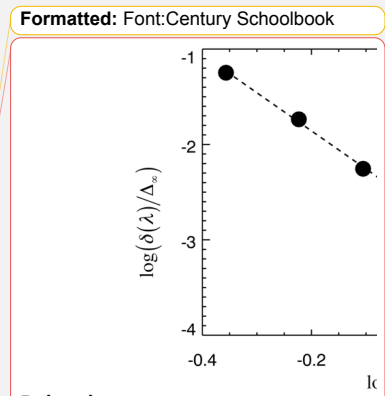


1

2 **Fig. 5.** Conceptual visualization of the mechanism of horizontal photon transport.

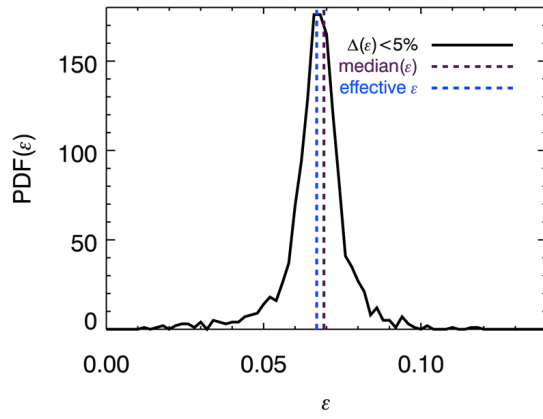


1
 2 **Fig. 6.** (a) An example of the linear regression between $\log \frac{\delta(\lambda)}{H_\infty}$ versus $\log \frac{\lambda}{\lambda_0}$, from which the
 3 values of x and ϵ can be derived. (b) The scatter plot of x versus ϵ for all pixels, joint PDFs $p(x, \epsilon)$
 4 (contours) as well as the marginal PDFs $p(x)$ and $p(\epsilon)$ (histograms). The peak of $p(x, \epsilon)$, and thus
 5 the most likely $\{x, \epsilon\}$ values for the cloud field is located at $\{3.85, 0.065\}$, and the domain-
 6 averaged values are $\{3.91, 0.070\}$.



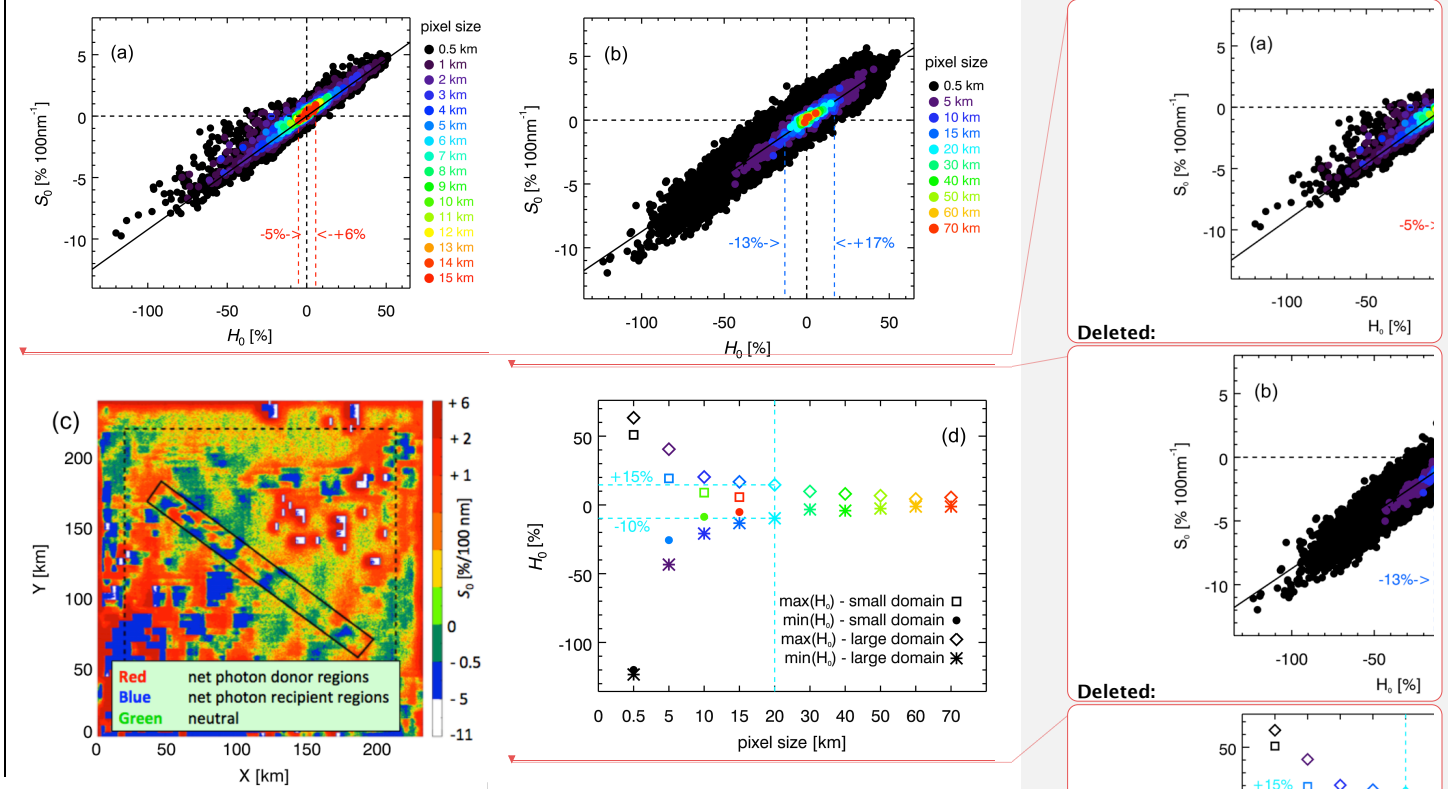
Deleted:
Comment [1]: On the y-axis, we should have H_∞ in denominator, not Δ_∞

values

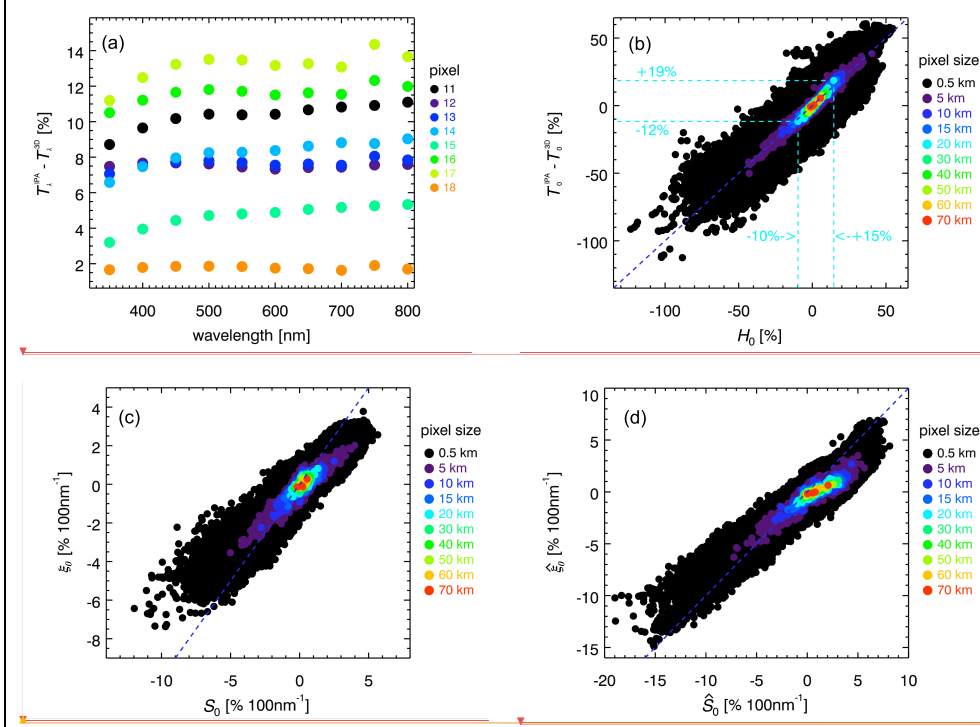


1
 2 **Fig. 7.** PDF of ε for all pixels with $\Delta(\varepsilon) < 5\%$, median (purple dashed line), and domain-wide
 3 *effective* ε derived from regression of S_0 vs. H_0 (blue dashed line).

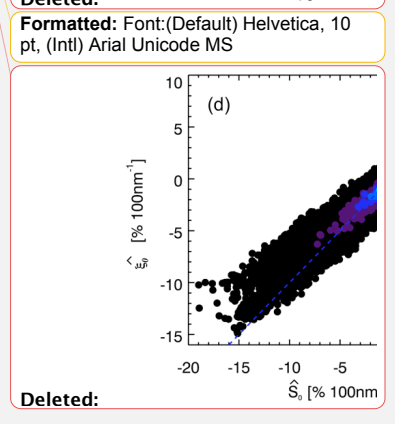
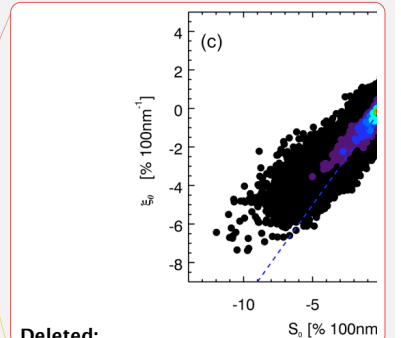
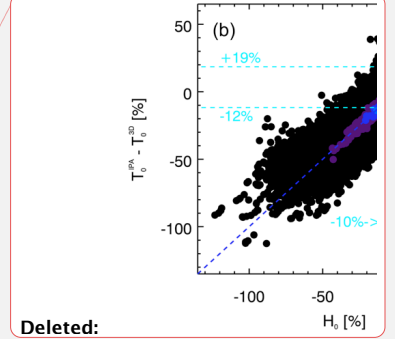
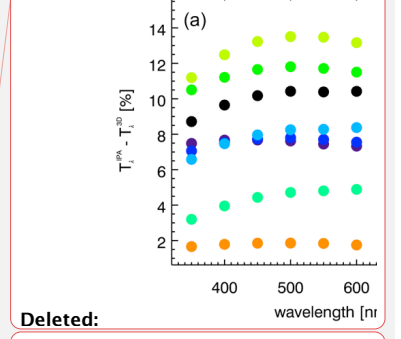
Deleted: H_∞

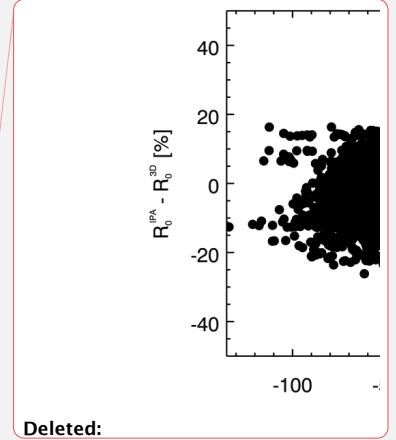
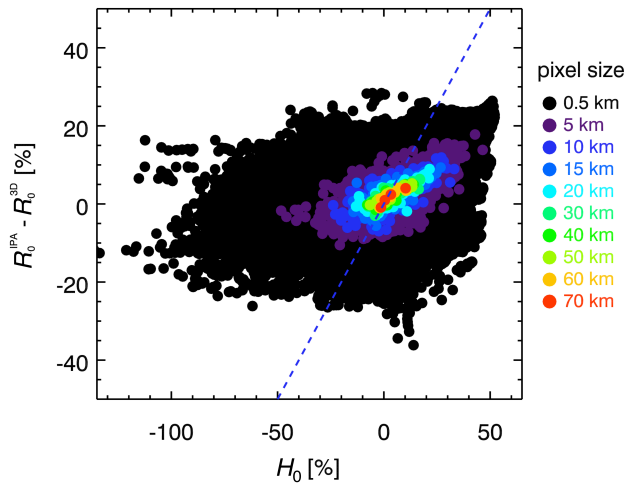


1 **Fig. 8.** Scatter plot of S_0 versus H_0 as obtained from linear regression of Eq. (12) for (a) the small
2 domain from Fig. 1 and (b) the large-scale domain from Fig. 2, spatially aggregated to different
3 scales, including the 20 km “super pixels” as highlighted in Fig. 2 (red squares). The dashed lines
4 indicate the range for 15 km pixels. (c) Spatial distribution of S_0 from (b). Red (blue) indicates
5 net photon “donor” (“recipient”) pixels, and green “neutral zones” ($H_\lambda \approx S_0 \approx 0$). (d) Dependence
6 of $\max(H)$ and $\min(H)$ on spatial aggregation scale (km). The color is the same as in (b).



1 **Fig. 9.** (a) Transmittance biases (IPA-3D transmittance) for the eight super-pixels from Fig. 2. (b)
 2 Correlation between net horizontal photon transport from Fig. 8b and transmittance bias for
 3 multiple spatial aggregation scales. The dashed lines indicate the range of variability for 20 km
 4 super-pixel size. (c) Correlation of the *slopes* of the quantities from (b). (d) Same as (c), but for a
 5 bracket from the surface to cloud top, rather than the cloud layer only.





1
 2 **Fig. 10.** H_0 is only weakly correlated with reflectance biases ΔR_0 (IPA-3D reflectance) at scales
 3 below 15 km, which means that, statistically, biases introduced by horizontal photon transport
 4 propagate primarily into transmittance, not albedo. This changes for larger scales.

5
 6